Full title: MARCKS mediates vascular contractility through regulating interactions between voltage-gated Ca^{2+} channels and PIP_2

Authors: Kazi S. Jahan[1], Jian Shi[2], Harry Z.E. Greenberg[1], Sam Khavandi[1], Miguel Martin-Aragon Baudel[3], Vincenzo Barrese[4], Iain A. Greenwood[1] and Anthony P. Albert[1]

Author affiliations:

[1]Vascular Biology Research Centre, Molecular and Clinical Research Institute, St. George's, University of London, Cranmer Terrace, London, UK, SW17 0RE

[2]Leeds Institute of Cardiovascular and Metabolic Medicine, Faculty of Medicine and Health, University of Leeds, Leeds, UK, LS2 9JT

[3]Department of Pharmacology, University of California, 451, Health Sciences Drive, Suite 3503, Davis, CA, 95615, USA

[4]Department of Neurosciences, Reproductive Sciences and Dentistry, University of Naples Federico II, Corso Umberto I, 40, 80138, Napoli, NA, Italy

Corresponding author: Professor Anthony Albert, Vascular Biology Research Centre, Molecular and Clinical Research Institute, St. George's, University of London, Cranmer Terrace, London, SW17 0RE, email: aalbert@sgul.ac.uk, Tel: 020 8725 5608

Abstract

Phosphatidylinositol 4,5-bisphosphate (PIP_2) acts as substrate and unmodified ligand for Gq-protein-coupled receptor signalling in vascular smooth muscle cells (VSMCs) that is central for initiating contractility. The present work investigated how PIP_2 might perform these two potentially conflicting roles by studying the effect of myristoylated alanine-rich C kinase substrate (MARCKS), a PIP_2-binding protein, on vascular contractility in rat and mouse mesenteric arteries. Using wire myography, MANS peptide (MANS), a MARCKS inhibitor, produced robust contractions with a pharmacological profile suggesting a predominantly role for L-type (CaV1.2) voltage-gated Ca^{2+} channels (VGCC). Knockdown of MARCKS using morpholino oligonucleotides reduced contractions induced by MANS and stimulation of α_1-adrenoceptors and thromboxane receptors with methoxamine (MO) and U46619 respectively. Immunocytochemistry and proximity ligation assays demonstrated that MARCKS and CaV1.2 proteins co-localise at the plasma membrane in unstimulated tissue, and that MANS and MO reduced these interactions and induced translocation of MARCKS from the plasma membrane to the cytosol. Dot-blots revealed greater PIP_2 binding to MARCKS than CaV1.2 in unstimulated tissue, with this binding profile reversed following stimulation by MANS and MO. MANS evoked an increase in peak amplitude and shifted the activation curve to more negative membrane potentials of whole-cell voltage-gated Ca^{2+} currents, which were prevented by depleting PIP_2 levels with wortmannin. This present study indicates for the first time that MARCKS is important regulating vascular contractility and suggests that disinhibition of MARCKS by MANS or vasoconstrictors may induce contraction through releasing PIP_2 into the local environment where it increases voltage-gated Ca^{2+} channel activity.

Keywords: MARCKS, PIP_2, voltage-gated Ca^{2+} channels, contractility

1. Introduction

It is well-established that phosphatidylinositol 4,5-bisphosphate (PIP_2) acting as a substrate for Gq-protein-coupled receptor signalling in vascular smooth muscle cells (VSMCs) has a central role in vasoconstrictor-mediated contractility [1,2]. Gq-protein receptor-mediated phospholipase C (PLC) activity leads to PIP_2 hydrolysis and generation of inositol 1,4,5-trisphosphate (IP_3) and diacylglycerol (DAG) which drive multiple pathways that increase intracellular Ca^{2+} concentration to induce contraction. In particular, IP_3-mediated Ca^{2+} release from sarcoplasmic reticulum stores and DAG-mediated signal transduction pathways regulate an array of cation, Cl^-, and K^+ channel subtypes to induce membrane depolarisation and activation of voltage-gated Ca^{2+} channels (VGCC) to produce Ca^{2+} influx and contraction [1,2].

There is also considerable evidence that, in addition to its classical role as a substrate for Gq-mediated PLC activity, PIP_2 acts as an unmodified ligand to regulate proteins involved in modulating vascular contractility including ion channels involved in regulating membrane potential and VGCC activity [3-10]. This raises an important question in vascular biology; how can PIP_2 act as both substrate and unmodified ligand to regulate different cellular pathways involved in regulating contractility? An explanation is the existence of independent pools of PIP_2, produced through localised formation and/or sequestration of PIP_2 at the plasma membrane [11]. Sequestration is an attractive hypothesis as this would allow PIP_2 to be retained in the local environment, thus preventing locally formed PIP_2 from rapidly diffusing away from its site of action [11,12]. There are several natively unfolded proteins which permit electrostatic interactions with PIP_2 and therefore sequestration, such as myristoylated alanine-rich C kinase (MARCKS), growth-associated protein 43 (GAP43), and cytoskeleton-associated protein 23 (CAP23) [13,14]. These proteins are proposed to act as PIP_2 buffers or PIPmodulins to release PIP_2 into the local environment following stimulation, allowing this source of PIP_2 to act as an unmodified ligand [11]. Hence PIP_2 sequestration proteins may have important roles in regulating vascular contractility by controlling PIP_2-mediated cellular processes. To date there have been no studies on the effect of PIP_2 sequestration proteins on vascular contraction, and therefore the present study investigates the role of MARCKS in such a function. MARCKS was chosen for this study since it is a ubiquitously expressed protein whereas GAP43 and CAP23 are mainly found in neurones [13,14].

Much is known about the chemical properties and cellular processes that regulate MARCKS but relatively little is known about the function of this PIP_2-binding protein, although it has been associated with neuronal development, cell migration and proliferation, and secretary pathways [15-25]. MARCKS structure contains two important regions, a myristoylated N-terminal region which weakly anchors it to the plasma membrane, and an effector domain containing a sequence of basic amino acids which form electrostatic interactions with PIP_2 that provide further stability at the plasma membrane. The effector domain also acts as a protein kinase (PKC) substrate and a calmodulin

(CaM)-binding region, with PKC-dependent phosphorylation and CaM binding both reducing electrostatic interactions with PIP_2, leading to PIP_2 release into the local environment and MARCKS to be translocated to the cytosol. These properties define MARCKS as a reversible PIP_2 buffer, which can provide spatial sequestration and release of PIP_2 to allow targeted function.

Several studies have shown that MARCKS is expressed in VSMCs where it has been proposed to have diverse functions including regulating PKC and CaM signalling [26], upregulation in neointima hyperplasia involving cell migration and proliferation [27-29], and modulation of TRPC1 channel activity [30]. However, there have been no studies on the role of MARCKS in regulating vascular contractility, and therefore this was the aim of the present work. To achieve this, we investigated the effect of the selective MARCKS inhibitor, MANS peptide (MANS), and knockdown of MARCKS expression using morpholino oligonucleotide technology [31,32]. MANS is a 24 amino acid sequence that corresponds to the initial N-terminal myristoylated region of MARCKS [33,34]. As such the MANS competes with endogenous MARCKS for binding to the plasma membrane, which leads to MARCKS being translocated into the cytosol and whilst releasing PIP_2 into the local environment. In addition, the hydrophobic myristate moiety means MANS is highly cell permeant. MANS has been used in several studies to reveal the role of MARCKS in mediating mucus secretion in the airways [33,34], immune cell degranulation [35,36], amylase release [37], and lung cancer metastasis [38].

The present study provides the first evidence that MARCKS acting as a plasma membrane PIP_2 buffer has an important role in regulating vascular contractility. Our findings suggest that disinhibition of MARCKS by MANS or vasoconstrictors may induce contraction through releasing PIP_2 into the local environment where it increases voltage-gated Ca^{2+} channel activity. These hypotheses provide provocative novel ideas on cellular mechanisms governing vascular contraction, which are likely to have important implications for understanding physiological and pathological processes.

2. Methods

An expanded Methods sections is provided in the supplementary data.

2.1 Animals

All animal procedures were carried out in accordance with guidelines laid down by St George's, University of London Animal Welfare Committee and conform with the principles and regulations described by the Service Project Licence: 70/8512. Male Wistar rats (8-12 weeks) and 129-SV mice (6-9 weeks) were used for the purpose of this study. Rats were supplied from Charles River, UK and 129-SV mice were bred in the Biological Research Facility at St George's, University of London. Animals were housed and maintained in standard sized plastic cages, with a 12 h light-dark cycle, ambient room temperature of 18-20^{o}C, relative humidity of approximately 50%, and water and lab rodent diet (Specialist Dietary Services, UK) available *ad libitum*. Animals were culled by cervical

dislocation in accordance with the UK Animals Scientific Procedures Act of 1986 and as revised by European Directive 2010/63/EU. Mesenteric arteries were dissected and cleaned of adherent fat in physiological salt solution containing (mM): 126 NaCl, 6 KCl, 10 Glucose, 11 HEPES, 1.2 $MgCl_2$, and 1.5 $CaCl_2$, with pH adjusted to 7.2 with 10 M NaOH. Mouse mesenteric arteries were used for wire myography, mouse IP_3 ELISA assay and proximity ligation assays. Rat mesenteric arteries were used when a greater yield of protein from tissue lysates or single VSMCs following tissue dispersal were required for better experimental efficiency such as transfection for imaging PLC activity, dot-blots and electrophysiological recordings.

2.2 Western Blotting

Mouse and rat mesenteric arteries were homogenised with radio immunoprecipitation assay lysis buffer containing a protease inhibitor cocktail (Santa Cruz, USA) (see supplementary data for more details). Samples were then loaded onto SDS-PAGE gels (4-12% Bis-Tris, Invitrogen, UK), subjected to electrophoresis, and then transferred onto a polyvinylidene fluoride membrane (Amersham Biosciences, UK). The membrane was then probed with an anti-MARCKS antibody (1:100; SC-6455, Santa Cruz, USA). Protein bands were visualized with a horseradish peroxidase-conjugated secondary antibody and enhanced chemiluminescence reagents (Pierce Biotechnology, USA) for 1 min and exposed to photographic films (Amersham Biosciences, UK).

2.3 Immunocytochemistry

Freshly dispersed VSMCs (see supplementary data for more details) were fixed with 4% (w/v) paraformaldehyde for 15 min and permeabilised with PBS containing 0.25% (v/v) Triton X-100 for 10 min at room temperature. Cells were then treated with phosphate-buffered saline (PBS) containing 1% (w/v) bovine serum albumin (BSA) for 1 h at room temperature, to block non-specific binding of antibodies. Immunostaining was performed using an anti-MARCKS primary antibody (1:100; SC-6455, Santa Cruz, USA) and/or anti-CaV1.2 primary antibody (1:100; ACC-003, Alomone, Israel) overnight at 4°C. Cells were then washed and incubated with a 488 fluorophore-conjugated donkey anti-goat secondary antibody (1:1000; A-11055, Alexa Fluor, UK) for 1 h at room temperature. Unbound secondary antibodies were removed by washing with PBS, and nuclei were labelled with 4, 6-diamidino-2-phenylindole (DAPI) mounting medium (Sigma, UK). Control experiments were performed by replacing primary antibody with goat serum (1:100; Sigma, UK) or omitting either primary or secondary antibodies. Cells were imaged using a Zeiss LSM 510 laser scanning confocal microscope (Carl Zeiss, Germany).

2.4 Isometric Tension Recordings

Segments of mouse superior mesenteric artery of about 2 mm in length were mounted on a wire myograph (Danish Myo Technology, Denmark) and endothelium was removed by rubbing the intima with a human hair. Vessel segments were bathed in Krebs solution containing (mM): 118.4 NaCl,

4.69 KCl, 1.18 $MgSO_4$, 1.22 KH_2PO_4, 25 $NaHCO_3$, 10 glucose and 2 $CaCl_2$, maintained at 37°C and constantly aerated with 95% O_2 and 5% CO_2. Vessel segments were then normalised to 90% of the internal circumference predicted to occur under a transmural pressure of 100 mmHg [39]. Vessel segments were then equilibrated for 30 min and assessed for vessel viability with 60 mM KCl for 5 min. Endothelium integrity was then assessed by stably pre-contracting vessels with 10 μM methoxamine (MO) followed by 10 μM carbachol (CCh). Carbachol-induced relaxation of <10% indicated successful removal of the endothelium. Vessels were then equilibrated for 10 min before the experimental protocol (see supplementary data for more details).

2.5 Morpholino-mediated MARCKS Knockdown

10 μM MARCKS-targeted (5'-GCACCCATGCTGGCTTCTTCAACAA-3') or scrambled morpholino (5'-GCACCgATcCTcGCTTgTTgAACAA) oligonucleotides (Gene Tools Inc., USA) were mixed with Lipofectamine 2000 (Life Technologies, UK) in Opti-MEM (Life Technologies, UK) and left at room temperature for 2 h. The Opti-MEM mix was then added to Dulbecco's modified Eagle's medium (DMEM)/Nutrient Mixture F-12 (Life Technologies, UK), containing 1% Penicillin-Streptomycin (Sigma, UK), and mouse superior mesenteric arteries were placed in this solution at 37°C for 48 h. Successful delivery of morpholino antisense oligonucleotides was assessed using an Olympus 1 × 60 fluorescence inverted microscope (Olympus, UK) with a Hamamatsu C4742-95 digital camera and motorized stage (Hamamatsu Protonics, UK). Successful knock-down of the protein and selectivity of MARCKS-targeted morpholino oligonucleotides were assessed by western blotting and immunocytochemical staining.

2.6 Transfection of PIP_2 Biosensors

GFP-PLCδ-PH was transfected into freshly dispersed rat mesenteric artery VSMCs by electroporation using Nucleofector™ Technology (Lonza, USA) as per manufacturer's instructions (see supplementary data for more details). Following electroporation, cells were incubated at 37°C in 95% O_2 and 5% CO_2 in a humidified incubator for 48 h before being imaged. Transfected cells were imaged at 37°C in 95% O_2 and 5% CO_2 in a humidified chamber using a Nikon AR1 inverted confocal microscope and associated software (Nikon Instruments, UK). Excitation was produced by a 488 laser. Final images were produced using PowerPoint (Microsoft XP; Microsoft, USA). Cell culture media contained: Ca^{2+} free DMEM supplemented with 1% fetal bovine serum (FBS), 1% Penicillin-Streptomycin, 2.5 mM L-Glutamine, 1 mM sodium pyruvate and 1 μM wortmannin. 1% FBS was used to maintain VSMC contractile phenotype and 1 μM wortmannin was used to prevent contraction of VSMCs following pre-treatment with MANS or MO, which prevents accurate imaging (as shown previously) [40,41].

2.7 Dot-Blots

Rat mesenteric artery segments were dissected, divided into three, and pre-treated with distilled water, 100 μM MANS, or 10 μM MO for 20 min at room temperature before extraction of protein (see supplementary data for more details). Next, 500 μg of tissue lysate was immunoprecipitated (see supplementary data for more details) with either an anti-MARCKS (SC-6455, Santa Cruz, USA) or anti-CaV1.2 primary antibody (ACC-003, Alomone, Israel). Then, 15 μl of immunoprecipitated rat mesenteric artery tissue lysate was blotted on nitrocellulose membranes (Amersham Biosciences, UK) and allowed to dry before being blocked in 5% (w/v) milk powder in 0.05% (v/v) PBST. Membranes were then incubated with an anti-PIP_2 antibody (1:200; SC-53412, Santa Cruz, USA) overnight at 4°C. Visualization was performed with a donkey anti-mouse (1:10,000; LI-COR Biotechnology, UK) fluorescently-conjugated secondary antibody, and imaged on the Odyssey Infrared Imaging System (LI-COR Biotechnology, UK). Blot intensities were analyzed with Image Studio, (version 3.0; LI-COR Biotechnology, UK).

2.8 Whole-cell recording

Whole-cell patch clamp voltage-clamp and current clamp recordings were conducted on freshly dispersed rat mesenteric artery VSMCs. In voltage-clamp studies, VGCC activity was evoked by applying 300 ms voltage steps from -80 mV to +40 mV at 10 mV intervals every 30 s from a holding potential of -60 mV. A control current-voltage (I/V) relationship curve was recorded before 100 μM MANS peptide was added to the extracellular solution in the presence or absence of 20 μM wortmannin, and then 3 μM nicardipine was used to confirm VGCC channel activity. The extracellular solution contained (mM): 110 NaCl, 1 CsCl, 10 $BaCl_2$, 1.2 $MgCl_2$, 10 glucose, 10 HEPES, 0.1 DIDS, 0.1 $GdCl_2$, adjusted to pH 7.4 with 10 M NaOH. The internal patch pipette solution contained (mM): 135 CsCl, 2.5 Mg-ATP, 0.1 GTP, 10 HEPES, 10 EGTA, adjusted to pH 7.2 with 10 M CsOH. In current clamp studies, membrane potential was recorded using an extracellular solution contained (mM): 126 NaCl, 6 KCl, 10 Glucose, 11 HEPES, 1.2 $MgCl_2$, and 1.5 $CaCl_2$, with pH adjusted to 7.2 with 10 M NaOH and an internal patch pipette solution contained (mM): 126 KCl, 5 NaCl, 2.5 Mg-ATP, 0.1 GTP, 10 HEPES, 1 BAPTA, adjusted to pH 7.2 with 10 M CsOH. Both voltage-clamp and current clamp recordings were conducted once the access resistance was <20 MΩ, filtered at 1 kHz, and sampled at 5 kHz. All recordings were made at room temperature.

2.9 Data Analysis

All data is expressed as mean ± standard error of mean for corresponding number (*n*) of animals. All statistical analysis was conducted using GraphPad Prism software (Version 7.04, GraphPad, USA). A *p* value of less than 5% ($p<0.05$) was considered statistically significant.

2.10 Materials

All chemicals and drugs were purchased from Sigma-Aldrich (Sigma Chemical Co., Poole, UK) or Tocris (Tocris Biosciences, Bristol, UK). MANS peptide (MANS) (Genemed Synthesis, USA) is a cell-permeable synthetic peptide that is identical to the first 24 amino acids of the MARCKS N-terminus [33,34] and contains the N-terminus myristic moiety (MA-GAQFSKTAAKGEAAAERPGEAAVA, MA= N-terminal myristate). GFP-PLCδ-PH was a gift from Professor Tobias Meyer (Plasmid identification #21179; Addgene, USA). Drugs were dissolved in distilled water or dimethyl sulfoxide (DMSO).

3. Results

3.1 MARCKS is expressed in mesenteric artery VSMCs

In our initial experiments we investigated the expression of MARCKS in tissue lysates and freshly isolated VSMCs from mouse and rat mesenteric arteries. Fig. 1A shows that western blot analysis revealed a single protein band of about 60 kDa following immunoblotting with an anti-MARCKS antibody, and Fig. 1B illustrates that distribution of MARCKS staining using the same anti-MARCKS antibody was predominantly located at, or close to, the plasma membrane of VSMCs using immunocytochemstry. These findings indicate that MARCKS is expressed in mesenteric artery, and that it may have a functional role at the plasma membrane of VSMCs.

3.2 MANS peptide induces vascular contractility

To investigate the role of MARCKS on vascular contractility we compared the effect of the selective MARCKS inhibitor, MANS peptide (MANS, see Introduction and Methods for peptide details) [33,34] with the α_1-adrenoceptor agonist methoxoamine (MO) on isometric tension recordings from segments of mouse mesenteric artery using wire myography. Fig. 2 shows that bath applications of MO and MANS induced concentration-dependent increases in contractility, with MANS having a greater effective half maximal concentration (EC_{50}) and maximal effect (E_{Max}) than MO of about 2-fold and 30% respectively. Contractile responses to both MO and MANS were sustained during continued application for 30 min and were reproducible following multiple cycles of bath application and washing (Fig. S1). These results suggest that MARCKS exerts an inhibitory action on contraction in unstimulated vessels, and that removal of this inhibition action by MANS induces vascular contractility in the absence of any receptor stimulation. The potential physiological importance of MARCKS on contractility is highlighted by the equivalence of contractions produced by MANS and stimulation of the α1-adrenoceptor-mediated vasoconstrictor pathway by MO.

3.3 Effect of reducing MARCKS expression on MANS- and vasoconstrictor-evoked contractility

To investigate the selectivity of MANS and provide further evidence that MARCKS regulates vascular contractility, we examined the effect of reducing MARCKS expression on MANS- and

vasoconstrictor-evoked contractility using morpholino oligonucleotide technology previously used to investigate other proteins in vascular contractility [31,32] (see Methods for oligomer details).

In initial experiments, we tested whether MARCKS-targeted morpholino oligomers reduce MARCKS expression. Fig. S2 shows that fluorescein-tagged morpholino oligonucleotides were successfully transfected into segments of mouse mesenteric artery after 48 hr, and that tissue lysates from vessels pre-treated with MARCKS-targeted compared to scrambled sequence oligomers had significantly reduced MARCKS expression by over 50%. Fig. S4 also shows that distribution of MARCKS staining at, or close to, the plasma membrane of VSMCs was reduced following pre-treatment of vessels with MARCKS-targeted oligomers. In control experiments, Fig. S2 shows that expression of α-tubulin or total protein levels were not altered by MARCKS-targeted oligomers. In additional control experiments, we examined the effect of MARCKS-targeted oligomers on expression levels of L-type (CaV1.2) VGCCs, as activation of these channels are known to be important for initiating vascular contractility [42-45]. Figs. S3 and S4 show that expression of CaV1.2 protein levels and distribution of CaV1.2 staining at, or close to, the plasma membrane of VSMCs was not altered in vessels pre-treated with MARCKS-targeted compared to scrambled oligomers. These results indicate that MARCKS-targeted oligomers produced substantial reduction of MARCKS expression but did alter α-tubulin, total protein and CaV1.2 expression levels.

Fig. 3 and Fig. S5 show that the MANS-evoked contractions of mouse mesenteric arteries pre-treated with scrambled oligomers for 48 h had similar mean EC_{50} and E_{max} values to those obtained from vessels recorded from on the same day of isolation (Fig. 2). Fig. 3 and Fig. S5 also show that, although the resting tension of mouse mesenteric artery segments was not altered with pre-treatment of MARCKS-targeted compared to scrambled oligomers, MANS-induced contractions were significantly reduced by MARCKS-targeted oligomers, with mean EC_{50} and E_{max} values increased by about 3-fold and reduced by over 50% respectively.

Interestingly, Fig. 4 and Fig. S5 also show that contractions of mouse mesenteric artery evoked by MO and the thromboxane receptor agonist U46619 were inhibited in vessels pre-treated with MARCKS-targeted compared to scrambled oligomers, with mean EC_{50} and E_{max} values increased by about 3-fold and reduced by over 50% respectively.

It is possible that MARCKS-targeted oligomers reduce contractility by inhibiting the activity of VGCCs and/or interfering with the Ca^{2+}-dependent contractile apparatus involving Ca^{2+}-CaM, myosin light chain kinase (MLCK), actin and myosin. Therefore, in control experiments, we investigated the effect of MARCK-targeted oligomers on contractions induced by high concentrations of KCl which induce contractility by producing membrane depolarisation, activation of VGCCs, Ca^{2+} influx and contraction and also by the Ca^{2+} ionophore ionomycin that causes Ca^{2+} influx independently of stimulation of

plasmalemmal receptors or activation of VGCCs. Fig. S6 shows that contractions induced by bath application of 60 mM and 120 mM KCl and 3 μM ionomycin were similar in vessels pre-treated with MARCKS-targeted and scrambled oligomers. These findings indicate that knockdown of MARCKS is unlikely to reduce MANS- and vasoconstrictor-evoked contractility by blocking VGCC activity or decreasing the ability of vessels to contract.

These results provide compelling evidence that MANS increases vascular contractility by acting via MARCKS and indicates that MARCKS is likely to have an important role in vasoconstrictor-mediated contraction.

3.4 MANS-induced vascular contractility is inhibited by L- and T-type VGCC blockers

In the next series of experiments, we investigated possible mechanisms involved in mediating MANS-induced contractions, to provide an insight into how MARCKS may regulate vascular contractility. We therefore investigated the effect of L- (CaV1.2) and T-type (CaV3.1/3 VGCC blockers on MANS-induced contraction of mouse mesenteric artery as both these VGCCs are thought to play a central role in mediating vascular contractility [42-45]. Fig. 5 and Fig. S7 show that co-application of the L-type channel blockers nicardipine, nifedipine and amlodipine or the T-type channel blockers mibefradil, NNC 55-0396 and Ni^{2+} produced concentration-dependent inhibition of pre-contracted vascular tone induced by a near maximal concentration of MANS (100 μM). All blockers could produce 100% relaxation. These findings suggest that vascular contractility induced by inhibition of MARCKS requires activation of VGCCs, which may involve both L- and T-type channel subtypes.

3.5 MANS has little effect on PLC activity or membrane potential

A potential hypothesis to explain why MANS induces contractility via VGCCs is that by inhibiting MARCKS it causes MARCKS to release PIP_2, which then is available to drive PLC activity and subsequent downstream stimulation of VGCCs. We explored this idea by studying the effect of MANS on PLC activity by transfecting rat mesenteric artery VSMCs primary cultured in low serum conditions (see Methods) with GFP-PLCδ-PH, a fluorescent biosensor with a high affinity for PIP_2 and IP_3 [46] and then recording signal changes in fluorescent intensity units at, or close to, the plasma membrane (Fm) and within the cytosol (Fc) as previously described [40,41].

Fig. 6 shows that in unstimulated VSMCs, GFP-PLCδ-PH signals were predominantly located at the plasma membrane with a mean Fm:Fc ratio of about 15, as expected when PIP_2 is mainly located at the plasma membrane and there is limited cytosolic IP_3. Fig. 6 illustrates that bath application of 100 μM MANS for 10 min failed to alter this signal distribution, whereas 10 μM MO induced translocation of GFP-PLCδ-PH signals to the cytosol that resulted in reduction of the mean Fm:Fc ratio by over 90%. These MO-induced signal changes are likely to represent PLC-mediated PIP_2

hydrolysis at the plasma membrane and subsequent generation of cytosolic IP_3 as previously described [40,41]. In support of these data, Fig. S8 shows that MO but not MANS altered PIP_2 levels at the plasma membrane measuring using the PIP_2-specific reporter GFP-tubby [46], as expected if MO induced PLC activity and MANS did not. Moreover, Fig. S9 shows that pre-treatment of mouse mesenteric artery segments with MANS did not significantly increase IP_3 levels measuring with an Elisa assay, whereas pre-treatment with MO induced about a 5-fold increase in IP_3 which is consistent with MO stimulating PLC activity. These results suggest that unlike MO, MANS is unlikely to produce significant effects on total PIP_2 levels at the plasma membrane or increase PLC activity,

Another possibility is that MANS induces contraction through producing membrane depolarisation which leads to stimulation of VGCCs and Ca^{2+} influx [1,2]. We investigated this idea by comparing the effects of MANS and MO on membrane potential using whole-cell patch clamp recording under current-clamp conditions. Figs. 7A and C show that in the presence of the bath and patch pipette solution conditions used (see Methods) VSMCs had a resting membrane potential of about -55 mV, and that bath application of MO induced a concentration-dependent membrane depolarisation with a maximum effect of over 30 mV at above 30 μM. In contrast, Fig. 7B and C show that bath application of 1-30 μM MANS failed to induce a change in membrane potential whereas 100 μM MANS evoked a small depolarisation of less than 10 mV. These results suggest that distinct from MO, MANS is unlikely to produce a significant effect on membrane potential in VSMCs.

3.5 MARCKS and CaV1.2 subunits are co-localised in VSMCs

The above data suggests, it is unlikely that MANS induces contraction via increasing PLC activity or evoking membrane depolarisation. We therefore examined if MARCKS may directly modulate VGCC activity. We addressed this idea by investigating whether MANS and MO modulate interactions between MARCKS and CaV1.2 subunits, which are proposed to be the predominant VGCC subtype involved in producing vascular contractility [42-45] and are likely to be involved in MANS-induced contractility (Fig. 5 and Fig. S7).

Fig. 8 show that immunocytochemical staining for MARCKS and CaV1.2 were mainly located at, or close to, the plasma membrane of mouse mesenteric artery VSMCs in unstimulated cells, and that there was substantial co-localisation between these signals. Bath application of 100 μM MANS and 10 μM MO reduced expression of MARCKS near the plasma membrane which was accompanied by a noticeable increase in MARCKS expression within the cytosol. In contrast, MANS and MO failed to affect the expression distribution of CaV1.2. Furthermore, Fig. S10 shows that proximity ligation assays (PLA) produced robust puncta formation between MARCKS and CaV1.2 at, or close to, the plasma membrane of unstimulated mouse mesenteric artery VSMCs, which was reduced by over 70% following pre-treatment with 100 μM MANS and 10 μM MO.

These results suggest that MARCKS and CaV1.2 interact with each other in unstimulated VSMCs, and that these interactions are reduced by MANS and MO. Importantly, our data also suggest that reductions in MARCKS-CaV1.2 interactions by MANS and MO are associated with translocation of MARCKS from the plasma membrane to the cytosol.

3.6 MANS and MO alter interactions between PIP_2, MARCKS, and CaV1.2

Since MARCKS is a well-established plasma membrane PIP_2-binding protein or PIPmodulin [11], we investigated if the reduction in MARCKS-CaV1.2 interactions and translocation of MARCKS into the cytosol produced by MANS and MO were accompanied by changes in PIP_2 associated with these two molecules. Using immunoprecipitation and dot-blot methods as previously described [30], Fig. 9 shows that there was a greater signal for PIP_2 interactions with MARCKS than for PIP_2 with CaV1.2 in unstimulated rat mesenteric artery tissue lysates. Following pre-treatment of vessels with 100 μM MANS and 10 μM MO the strength of these signals was reversed, with greater binding observed between of PIP_2 and CaV1.2 than for PIP_2 and MARCKS.

3.7 MANS increase VGCC activity through a PIP_2-dependent mechanism

Our findings suggest that within MARCKS-CaV1.2 complexes, PIP_2 may be predominantly bound to MARCKS and not CaV1.2. However, upon stimulation with MANS and MO, MARCKS is translocated from the plasma membrane to the cytosol leading to release of PIP_2 that binds to CaV1.2. This suggests that inhibition of MARCKS induces vascular contractility by increasing VGCC activity through a PIP_2-dependent mechanism. We explored this idea by studying the effect of MANS on VGCC current activity using Ba^{2+} as the charge carrier in rat mesenteric artery VSMCs using whole-cell patch clamp recording under voltage-clamp conditions.

Fig. 10A show that applying 300 ms voltage pulses from -80 mV to +40 mV in 10 mV steps from a holding potential of -60 mV induced whole-cell inward currents which activated at about -60 mV, reached a peak amplitude at about +20 mV, and were inhibited by the VGCC blocker nicardipine. These characteristics are consistent with activation of whole-cell VGCC currents as previously described in VSMCs [47-50]. Bath application of 100 μM MANS produced a pronounced increase in nicardipine-sensitive whole-cell inward currents, shifting the mean activation curve to more negative membrane potentials and increasing mean peak amplitude by over 50%. Moreover, Fig. 10B show that pre-treatment of VSMCs with a high concentration of wortmannin (20 μM), a PI4/PI5 kinase inhibitor that leads to depletion of PIP_2 levels [51,52], did not affect the activation curve of whole-cell inward currents but did prevent MANS-induced negative shift in the mean activation curve and increase in mean peak amplitude. This suggests that PIP_2 is likely to mediate the excitatory effect of MANS on VGCC activity.

To provide evidence that wortmannin reduces PIP_2 levels, Fig. S11 shows that wortmannin reduced the plasma membrane signals of the highly selective PIP_2 biosensor GFP-Tubby and the PIP_2/IP_3 biosensor GFP-PLCδ-PH in rat mesenteric artery VSMCs. Moreover, Fig. S11 shows that total PIP_2 levels from tissue lysates of mouse mesenteric artery measured using dot-blot analysis was reduced by pre-treatment with wortmannin.

4. Discussion

The present study provides the first evidence that the PIP_2-binding protein MARCKS regulates vascular contractility and reveals its potentially important role in mediating vasoconstrictor-induced contractions. Our initial findings suggest that MARCKS regulates contraction by modulating the activity of VGCCs by PIP_2. These results identify novel cellular mechanisms involved in regulating vascular contractility, which are likely to have important consequences for future understanding of physiological and pathological vascular function.

4.1 MARCKS regulates vascular contractility

We show that MARCKS is expressed in mouse and rat mesenteric artery VSMCs, where it is predominantly distributed at, or close to, the plasma membrane. This is consistent with earlier studies from ferret portal vein [26], human coronary artery [27-29] and rabbit and mouse portal vein [30].

We used a well-established pharmacological intervention to investigate the role of MARCKS in vascular contractility. The selective MARCKS inhibitor, MANS, evoked robust, sustained and reproducible vascular contractions in mouse mesenteric arteries, which were equivalent to contractions induced by stimulation of α_1-adrenoceptors by methoxamine (MO) and thromboxane receptors by U46619. MANS is a selective inhibitory peptide, which corresponds to the myristoylated N-terminal region that anchors MARCKS at the plasma membrane and has been extensively used to investigate the function of MARCKS in many different preparations [33-36]. MANS is used at relatively high concentrations (up to 100 μM) as it acts by competing for endogenous MARCKS at the plasma membrane and MARCKS is thought to have a cellular concentration of about 10 μM (similar to the cellular concentration of PIP_2) [33,34]. Thus, MANS is used at 10-fold greater concentrations than endogenous MARCKS to produce sufficient inhibition.

To provide molecular evidence that the effects of MANS were not produced through off-target actions, we showed that reducing MARCKS expression levels and, distribution at, or close to, the plasma membrane with MARCKS-targeted morpholino oligonucleotides greatly inhibited MANS-evoked contractions. Contractions evoked by MANS and MO in vessels pre-treated with scrambled morpholino oligomers had mean EC_{50} and E_{max} values similar to values recorded in freshly isolated arteries, and MARCKS-targeted oligomers did not alter expression of α-tubulin or the expression and cellular distribution of CaV1.2 proteins. These results suggest that the transfection process is

unlikely to alter vasoconstrictor-mediated responses or involvement of MARCKS inferred through use of MANS, and importantly that MARCKS-targeted oligomers have selectivity against MARCKS. All these findings increase the validity to our approach. The lack of an effect of MARCKS-targeted oligomers on expression levels and cellular distribution of CaV1.2 is also of importance as we show that CaV1.2 is likely to be involved in MARCKS-evoked contractions (see below).

A significant result was that contractions induced by MO and U46619 were also substantially inhibited by MARCKS-targeted oligomers, with changes in EC_{50} and E_{max} values equivalent to those observed with MANS-evoked contractions. These striking findings pose an interesting conflict; why does pharmacological inhibition of MARCKS produce contractility whereas knockdown of MARCKS expression reduces vasoconstrictor-evoked contractility? These seemingly opposing data can be explained if MARCKS exerts an inhibitory effect on contractility in unstimulated vessels and that disinhibition of this action of MARCKS is required for MANS- and vasoconstrictor-mediated contractility. As such, disinhibition of this MARCKS inhibitory action in unstimulated vessels by acute application or MANS or vasoconstrictor agents (e.g. MO and U46619) induce contraction. However, following knockdown of MARCKS, MANS and vasoconstrictor-stimulated disinhibition of MARCKS is curtailed leading to a reduction in contraction. These ideas suggest is that disinhibition of MARCKS causing contraction is unlikely to be a pharmacological phenomenon but is an important physiological pathway which is necessary for vasoconstrictor-mediated contractility.

It is possible that MARCKS-targeted oligomers may have reduced MANS- and vasoconstrictor-mediated contractions by having non-selective effects on the activity of VGCCs and/or by reducing the ability of vessels to contract. However, this seems unlikely, contractions induced by KCl and ionomycin, which induce contractility through stimulating VGCCs and providing direct Ca^{2+} influx to activate Ca^{2+}-dependent contractile mechanisms respectively were similar in vessels transfected with scrambled and MARCKS-targeted oligomers. It might have been expected that knockdown of MARCKS would alter resting tension, produced in the normalisation process to represent a physiological blood pressure of 100 mmHg, but our results showed that resting tension was not different between vessels pre-treated with scrambled and MARCKS-targeted oligomers. This should perhaps be investigated in future experiments using pressure myography which may provide greater resolution.

In conclusion, these findings indicate that endogenous MARCKS has a pronounced inhibitory action on vascular contractility which can be modulated by direct inhibition of MARCKS and vasoconstrictor stimulation. MARCKS has previously been shown to regulate proliferation and migration of VSMCs and has been implicated in the progression of intima hyperplasia [27-29]. However, this is first time that MARCKS has been implicated in regulating contractility.

4.2 MANS evokes vascular contractility via activation of VGCCs

It is well-established that Ca^{2+} influx through activation of VGCCs plays a central role in mediated vascular contraction involving two VGCC subtypes, L-type (CaV1.2) and T-type (CaV3.1/3), with L-Type VGCCs considered to have the predominant role in initiating vasoconstrictor-mediated contraction [42-45]. Our results show that MANS-evoked contractions were inhibited by several proposed selective L-type and T-type VGCC blockers, with each agent able to produce complete relaxation. The IC_{50} values for the blockers against MANS-evoked contractions were relatively high compared to known values for these channel subtypes [53-57]. This may be due to the blockers being applied to pre-contracted vessels and not pre-incubated before contraction was induced and/or that multiple VGCC subtypes are involved. It is therefore difficult to accurately determine from these experiments if either or both L-type and T-type VGCCs are involved in mediating MANS-evoked contractions. A potential discrimination is provided by the effect of Ni^{2+}, reported to offer T-type VGCCs selectivity at concentrations less than 50 μM [55], which blocked MANS-evoked contractions with an IC_{50} of 250 μM suggesting a predominant role for L-type VGCC subtype. What is certain is that activation of VGCCs play a central role in the pathway whereby disinhibition of MARCKS by MANS induces contraction.

4.3 MARCKS regulates interactions between VGCCs and PIP_2

It is recognised that MANS, by competing with MARCKS at the plasma membrane, induces translocation of MARCKS from the plasma membrane to the cytosol that reduces electrostatic interactions between MARCKS and PIP_2 causing release of PIP_2 into the local environment [33,34]. We therefore considered that MANS may induce VGCC-mediated contractions by inducing a rise in PIP_2 levels, which acts as a substrate for PLC activity to induce contraction via the familiar phosphatidylinositol transduction pathway. In addition, MANS may also induce VGCCs and contraction by evoking a membrane depolarisation. However, MANS failed to alter the distribution of the PIP_2/IP_3 biosensor GFP-PLCδ-PH and PIP_2-specific reporter GFP-tubby and had little effect on membrane potential in VSMCs. This contrasts with stimulation of α_1-adrenoceptors, which induced a translocation of GFP-PLCδ-PH and GFP-tubby from the plasma membrane to the cytosol in VSMCs that is indicative of PLC activity [40,41], and induced a significant membrane depolarisation. These findings are further supported by previous evidence indicating that sequestered PIP_2 by MARCKS does not interfere with PLC activity [12,24].

We next focused on the possibility that MANS and MO induce contraction through regulating interactions between MARCKS, VGCCs, and PIP_2. We studied the L-type CaV1.2 subunit as this is considered the dominant VGCC involved in initiating vascular contractility by MANS from the pharmacological profile [42-45]. Using immunocytochemistry and PLA, we clearly show that MARCKS-CaV1.2 interactions are present in unstimulated VSMCs and that these associations occur at, or close to, the plasma membrane. In addition, MANS and MO both cause dissociation of

MARCKS-CaV1.2 interactions and MARCKS to translocate the cytosol. Moreover, we show that in unstimulated vessel segments PIP_2 was bound more to MARCKS than CaV1.2, but that this binding profile was reversed following pre-treatment with MANS and MO. These results are similar to earlier studies showing that the known inhibitors of MARCKS, CaM and PKC [15-26,30], and MO [30] lead to translocation of MARCKS from the plasma membrane to the cytosol, and that MO induces preferential changes in PIP_2 binding at MARCKS-TRPC1 interactions [30]. These findings provide further evidence that MANS induces vascular contractility by causing disinhibition of an endogenous MARCKS inhibitory pathway. Moreover, PIP_2 imaging with GFP-PLCδ-PH, GFP-tubby and dot-blots, indicate that redistribution of PIP_2 from MARCKS to CaV1.2 subunits and not changes in total PIP_2 levels may be an important step in this pathway.

To provide further context to our ideas that MARCKS regulates VGCCs via a PIP_2-dependent mechanism, MANS induced an increase in whole-cell VGCC currents in VSMCs through shifting the activation curve to more negative membrane potentials and augmenting mean peak amplitude. These MANS-mediated increases in VGCC currents were prevented by pre-treatment of VSMCs with wortmannin which depletes endogenous PIP_2 levels. This is consistent with studies showing that PIP_2 facilitates L-, T-, and P-type VGCC activity in overexpression systems [3-10]. High concentration of wortmannin (20 μM) depletes PIP_2 levels through inhibiting PI-4/PI-5 kinase-mediated PIP_2 synthesis (see Fig. S10) [4]. However, it should be noted that high concentrations of wortmannin is also likely to inhibit myosin light chain kinase (MLCK) and PI-3 kinase, and therefore due caution should be given to these results.

Taken together, the present work indicates that MARCKS regulates vascular contractility by modulating VGCC activity (see Fig. S12). In unstimulated VSMCs, MARCKS forms interactions with CaV1.2 and acts as a PIP_2 buffer or PIPmodulin [11] to sequester local PIP_2 levels that reduces PIP_2-mediated facilitation of VGCC activity. Disinhibition of MARCKS by MANS leads to dissociation of MARCKS-CaV1.2 interactions and translocation of MARCKS to the cytosol, which releases sequestered PIP_2 at the plasma membrane where it binds to and facilitates VGCC activity to promote contraction. In the future it will be important to identify if both L-type (CaV1.2) and T-type (CaV3.1/3) VGCC subtypes are involved, and whether pore-forming α subunits and auxiliary subunits such as β and $\alpha_2\delta$ contribute to these responses. Moreover, a detailed examination of exogenous PIP_2 and endogenous PIP_2 actions on VGCC activity is required using respectively: water soluble forms of PIP_2 such as diC8-PIP_2 and established techniques to deplete endogenous PIP_2 levels such as *Danio rerio* voltage-sensing phosphatase (DrVSP) and rapamycin-FRB/FKBP-5' phosphatase is required [58]. In the longer term it will be important to reveal the structure of PIP2-VGCC interaction sites.

4.4 Future implications for understanding cellular mechanisms regulating vascular contractility

Our findings reveal that α_1-adrenoceptor stimulation produced similar actions to MANS on MARCKS-CaV1.2 interactions, MARCKS translocation, and changes in PIP_2 binding to MARCKS and CaV1.2 (Fig. S12). In contrast, stimulation of α_1-adrenoceptors evoked a substantial membrane depolarisation of VSMCs whereas MANS had little effect on membrane potential. It is generally considered that stimulation of Gq-protein receptor-mediated pathways by vasoconstrictors induces contractility through inducing membrane potential depolarisation through modulation of ion channels such as cation, Cl^-, and K^+ channels which cause activation of VGCCs and Ca^{2+} influx [1,2,59]. The present study poses important questions about these established vasoconstrictor-mediated pathways by suggesting that, in addition to membrane depolarisation, these Gq-protein receptor-mediated pathways may also cause disinhibition of MARCKS to directly activate of VGGCs to produce contraction. Essentially, VGCCs become receptor-operated channels at the resting membrane potential through the facilitatory effect of PIP_2 released from MARCKS, which shifts the activation threshold of VGCCs to more negative membrane potentials. The idea that VGCCs may be receptor-operated channels and are activated independently of membrane depolarisation is not new, some 30 years ago, Nelson and colleagues presented evidence that vasoconstrictors activate VGCCs held at resting membrane potentials [60]. There is no doubt that this concept needs revisiting, such as does α_1-adrenceptor-induced contractions require MARCKS and are known Gq-protein receptor-mediated CaM and/or PKC pathways coupled to disinhibition of MARCKS and regulation of contractility [26,30]. Whatever the outcome of these future experiments, the present study provides the first evidence that MARCKS has a critical role in regulating vascular contractility and offers a potential new target for modulating contractility in treating cardiovascular disease.

Acknowledgements

None.

Sources of funding

This work was supported by a British Heart Foundation PhD Studentship to Kazi S. Jahan (FS/15/44/31570 to A.P.A.), and by the Biotechnological and Biological Scientific Research Council (BB/J007226/1 and BB/M018350/1 to A.P.A.).

Disclosures

None.

645 **References**

646 1. Gonzales AL, Earley S, Regulation of cerebral artery smooth muscle membrane potential by
647 Ca^{2+}-activated cation channels. Microcirculation 20 (2013) 337-47.
648 2. Liu Z, Khalil RA, Evolving mechanisms of vascular smooth muscle contraction highlight key
649 targets in vascular disease. Biochem. Pharmacol. 153 (2018) 91-122.
650 3. Wu L, Bauer CS, Zhen X, Xie C, Yang J, Dual regulation of voltage-gated calcium channels
651 by PtdIns(4,5)P_2. Nature 419 (2002) 947–952.
652 4. Suh BC, Hille B, Regulation of ion channels by phosphatidylinositol 4,5-bisphosphate. Curr.
653 Opin. Neurobiol. 15 (2005) 370–378.
654 5. Suh B-C, Kim D-I, Falkenburger BH, Hille B, Membrane-localized β-subunits alter the PIP_2
655 regulation of high-voltage activated Ca^{2+} channels. Proc. Natl. Acad. Sci. 109 (2012) 3161–3166.
656 6. Zhen X-G, Xie C, Yamada Y, Zhang Y, Doyle C, Yang J, A single amino acid mutation
657 attenuates rundown of voltage-gated calcium channels. FEBS Lett. 580 (2006) 5733–5738.
658 7. Suh B-C, Hille B, PIP_2 Is a Necessary Cofactor for Ion Channel Function: How and Why?
659 Annu. Rev. Biophys. 37 (2008) 175–195.
660 8. Falkenburger BH, Jensen JB, Dickson EJ, Suh B-C, Hille B, Phosphoinositides: lipid
661 regulators of membrane proteins. J. Physiol. 588 (2010) 3179–3185.
662 9. Suh B-C, Leal K, Hille B, Modulation of high-voltage activated Ca(2+) channels by membrane
663 phosphatidylinositol 4,5-bisphosphate. Neuron. 67 (2010) 224–238.
664 10. Hille B, Dickson EJ, Kruse M, Vivas O, Suh B-C, Phosphoinositides regulate ion channels.
665 Biochim. Biophys. Acta. 1851 (2015) 844–856.
666 11. Gamper N, Shapiro MS. Target-specific PIP_2 signalling: how might it work? J. Physiol. 582
667 (2007) 967–975.
668 12. Wang J, Gambhir A, Hangyás-Mihályné G, Murray D, Golebiewska U, McLaughlin S, Lateral
669 sequestration of phosphatidylinositol 4,5-bisphosphate by the basic effector domain of myristoylated
670 alanine-rich C kinase substrate is due to nonspecific electrostatic interactions. J. Biol. Chem. 277
671 (2002) 34401–34412.
672 13. McLaughlin S, Wang J, Gambhir A, Murray D, PIP_2 and proteins: Interactions, Organization,
673 and Information Flow. Annu. Rev. Biophys. Biomol. Struct. 31 (2002) 151–175.
674 14. McLaughlin S, Murray D, Plasma membrane phosphoinositide organization by protein
675 electrostatics. Nature 438 (2005) 605–611.
676 15. Arbuzova A, Murray D, McLaughlin S, MARCKS, membranes, and calmodulin: kinetics of
677 their interaction. Biochim. Biophys. Acta. 1376 (1998) 369–379.
678 16. Arbuzova A, Schmitz AAP, Vergères G, Cross-talk unfolded: MARCKS proteins. Biochem. J.
679 362 (2002) 1–12.
680 17. Blackshear PJ, The MARCKS family of cellular protein kinase C substrates. J. Biol. Chem.
681 268 (1993) 1501–1504.
682 16. Porumb T, Crivici A, Blackshear PJ, Ikura M, Calcium binding and conformational properties

683 of calmodulin complexed with peptides derived from myristoylated alanine-rich C kinase substrate
684 (MARCKS) and MARCKS-related protein (MRP). Eur. Biophys J. 25 (1997) 239–247.
685 18. Allen LA, Aderem A, Protein kinase C regulates MARCKS cycling between the plasma
686 membrane and lysosomes in fibroblasts. EMBO. J. 14 (1995) 1109–1121.
687 20. Hartwig JH, Thelen M, Rosen A, Janmey PA, Nairn AC, Aderem A, MARCKS is an actin
688 filament crosslinking protein regulated by protein kinase C and calcium-calmodulin. Nature 356
689 (1992) 618–622.
690 21. Wang J, Arbuzova A, Hangyás-Mihályné G, McLaughlin S, The effector domain of
691 myristoylated alanine-rich C kinase substrate binds strongly to phosphatidylinositol 4,5-
692 bisphosphate. J. Biol. Chem. 276 (2001) 5012–5019.
693 22. McLaughlin S, Aderem A, The myristoyl-electrostatic switch: a modulator of reversible
694 protein-membrane interactions. Trends Biochem. Sci. 20 (1995) 272–276.
695 23. McLaughlin S, Hangyás-Mihályné G, Zaitseva I, Golebiewska U, Reversible - through
696 calmodulin - electrostatic interactions between basic residues on proteins and acidic lipids in the
697 plasma membrane. Biochem. Soc. Symp. 72 (2005) 189–198.
698 24. Gambhir A, Hangyás-Mihályné G, Zaitseva I, Cafiso DS, Wang J, Murray D, Pentyala SN,
699 Smith SO, McLaughlin S, Electrostatic Sequestration of PIP_2 on Phospholipid Membranes by
700 Basic/Aromatic Regions of Proteins. Biophys. J. 86 (2004) 2188–2207.
701 25. Tzlil S, Murray D, Ben-Shaul A, The “electrostatic-switch” mechanism: Monte Carlo study of
702 MARCKS-membrane interaction. Biophys. J. 95 (2008) 1745–1757.
703 26. Gallant C, You JY, Sasaki Y, Grabarek Z, Morgan KG, MARCKS is a major PKC-dependent
704 regulator of calmodulin targeting in smooth muscle. J. Cell. Sci. 118 (2005) 3595–3605.
705 27. Monahan TS, Andersen ND, Martin MC, Malek JY, Shrikhande G V, Pradhan L, Ferran C,
706 LoGerfo FW, MARCKS silencing differentially affects human vascular smooth muscle and
707 endothelial cell phenotypes to inhibit neointimal hyperplasia in saphenous vein. Faseb. J. 23 (2009)
708 557–564.
709 28. Yu D, Makkar G, Dong T, Strickland DK, Sarkar R, Monahan TS, MARCKS Signaling
710 Differentially Regulates Vascular Smooth Muscle and Endothelial Cell Proliferation through a KIS-,
711 p27kip1-Dependent Mechanism. PLoS One. 10 (2015) e0141397.
712 29. Yu D, Gernapudi R, Drucker C, Sarkar R, Ucuzian A, Monahan TS, The myristoylated
713 alanine-rich C kinase substrate differentially regulates kinase interacting with stathmin in vascular
714 smooth muscle and endothelial cells and potentiates intimal hyperplasia formation. J. Vasc Surg. 70
715 (2019) 2021-2031.
716 30. Shi J, Birnbaumer L, Large WA, Albert AP, Myristoylated alanine-rich C kinase substrate
717 coordinates native TRPC1 channel activation by phosphatidylinositol 4,5-bisphosphate and protein
718 kinase C in vascular smooth muscle. Faseb. J. 28 (2014) 244–255.
719 31. Jepps TA, Carr G, Lundegaard PR, Olesen SP, Greenwood IA, Fundamental Role for the
720 KCNE4 Ancillary Subunit in Kv7.4 Regulation of Arterial Tone. J. Physiol. 593 (2015) 5325-5340.

32. Stott JB, Barrese V, Suresh M, Masoodi S & Greenwood IA, Investigating the Role of G Protein βγ in Kv7-Dependent Relaxations of the Rat Vasculature. Arterioscler. Thromb. Vasc. Biol. 38 (2018) 2091-2102.
33. Li Y, Martin LD, Spizz G, Adler KB, MARCKS Protein Is a Key Molecule Regulating Mucin Secretion by Human Airway Epithelial Cells in Vitro. J. Biol. Chem. 276 (2001) 40982–40990.
34. Singer M, Martin LD, Vargaftig BB, Park J, Gruber AD, Li Y, Adler KB, A MARCKS-related peptide blocks mucus hypersecretion in a mouse model of asthma. Nat. Med. 10 (2004) 193–196.
35. Takashi S, Park J, Fang S, Koyama S, Parikh I, Adler KB, A peptide against the N-terminus of myristoylated alanine-rich C kinase substrate inhibits degranulation of human leukocytes in vitro. Am. J. Respir. Cell. Mol. Biol. 34 (2006) 647-652.
36. Eckert RE, Neuder LE, Park J, Adler KB, Jones SL, Myristoylated alanine-rich C-kinase substrate (MARCKS) protein regulation of human neutrophil migration. Am. J. Respir. Cell. Mol. Biol. 42 (2010) 586-594.
37. Satoh K, Matsuki-Fukushima M, Qi B, Guo MY, Narita T, Fujita-Yoshigaki J, Sugiya H, Phosphorylation of myristoylated alanine-rich C kinase substrate is involved in the cAMP-dependent amylase release in parotid acinar cells. Am. J. Physiol. Gastrointest. Liver. Physiol. 296 (2009) G1382-G1390.
38. Chen C-H, Thai P, Yoneda K, Adler KB, Yang P-C, Wu R, A peptide that inhibits function of Myristoylated Alanine-Rich C Kinase Substrate (MARCKS) reduces lung cancer metastasis. Oncogene. 33 (2014) 3696–3706.
39. Mulvany MJ, Halpern W, Contractile properties of small arterial resistance vessels in spontaneously hypertensive and normotensive rats. Circ. Res. 41 (1977) 19–26.
40. Shi J, Miralles F, Birnbaumer L, Large WA, Albert AP, Store depletion induces Gαq-mediated PLCβ1 activity to stimulate TRPC1 channels in vascular smooth muscle cells. Faseb. J. 30 (2016) 702–715.
41. Shi J, Miralles F, Birnbaumer L, Large WA, Albert AP, Store-operated interactions between plasmalemmal STIM1 and TRPC1 proteins stimulate PLCβ1 to induce TRPC1 channel activation in vascular smooth muscle cells. J. Physiol. 595 (2017) 1039-1058.
42. Gollasch M, Nelson MT, Voltage-dependent Ca^{2+} channels in arterial smooth muscle cells. Kidney. Blood. Press. Res. 20 (1997) 355–371.
43. Cribbs LL, Vascular smooth muscle calcium channels: could “T” be a target? Circ. Res. 89 (2001) 560–562.
44. Cribbs LL, T-type Ca^{2+} channels in vascular smooth muscle: multiple functions. Cell Calcium 40 (2006) 221–230.
45. Kuo IY-T, Wölfle SE, Hill CE, T-type calcium channels and vascular function: the new kid on the block? J. Physiol. 589 (2011) 783–795.
46. Quinn K V, Behe P, Tinker A, Monitoring changes in membrane phosphatidylinositol 4,5-bisphosphate in living cells using a domain from the transcription factor tubby. J. Physiol. 586 (2008)

2855–2871.
47. Greenberg HZE, Jahan KS, Shi J, Vanessa Ho WS, Albert AP, The calcilytics Calhex-231 and NPS 2143 and the calcimimetic Calindol reduce vascular reactivity via inhibition of voltage-gated Ca^{2+} channels. Eur. J. Pharmacol. 791 (2016) 659–668.
48. Tang J, Li N, Chen X, Gao Q, Zhou X, Zhang Y, Liu B, Sun M, Xu Z, Prenatal Hypoxia Induced Dysfunction in Cerebral Arteries of Offspring Rats. J. Am. Heart. Assoc. 6 (2017) e006630.
49. Aaronson PI, Bolton TB, Lang RJ, MacKenzie I, Calcium currents in single isolated smooth muscle cells from the rabbit ear artery in normal-calcium and high-barium solutions. J. Physiol. 405 (1988) 57–75.
50. Cai Q, Zhu Z-L, Fan X-L, Whole-cell recordings of calcium and potassium currents in acutely isolated smooth muscle cells. World. J. Gastroenterol. 12 (2006) 4086–4088.
51. Downing GJ, Kim S, Nakanishi S, Catt KJ, Balla T, Characterization of a Soluble Adrenal Phosphatidylinositol 4-Kinase Reveals Wortmannin Sensitivity of Type III Phosphatidylinositol Kinases. Biochemistry. 35 (1996) 3587–3594.
52. Nakanishi S, Catt KJ, Balla T, A wortmannin-sensitive phosphatidylinositol 4-kinase that regulates hormone-sensitive pools of inositolphospholipids. Proc. Natl. Acad. Sci. 92 (1995) 5317–5321.
53. Hofmann F, Lacinová L, Klugbauer N, Voltage-dependent calcium channels: From structure to function. In: Reviews of Physiology, Biochemistry and Pharmacology, Volume 139. Berlin/Heidelberg: Springer-Verlag; 1999. p. 33–87.
54. Lacinová L, Hofmann F, Ca^{2+}- and voltage-dependent inactivation of the expressed L-type Cav1.2 calcium channel. Arch. Biochem. Biophys. 437 (2005) 42–50.
55. Lee JH, Gomora JC, Cribbs LL, Perez-Reyes E, Nickel block of three cloned T-type calcium channels: low concentrations selectively block alpha1H. Biophys. J. 77 (1999) 3034–3042.
56. Wu S, Zhang M, Vest PA, Bhattacharjee A, Liu L, Li M, A mibefradil metabolite is a potent intracellular blocker of L-type Ca(2+) currents in pancreatic beta-cells. J. Pharmacol. Exp Ther. 292 (2000) 939–943.
57. Kuo IY, Ellis A, Seymour V AL, Sandow SL, Hill CE, Dihydropyridine-Insensitive Calcium Currents Contribute to Function of Small Cerebral Arteries. J. Cereb. Blood. Flow. Metab. 30 (2010) 1226–1239.
58. Okamura Y, Murata Y, Iwasaki H, Voltage-sensing phosphatase: actions and potentials. J. Physiol. 587 (2009) 513–520.
59. Nelson MT, Patlak JB, Worley JF, Standen NB, Calcium channels, potassium channels, and voltage dependence of arterial smooth muscle tone. Am. J. Physiol. 259 (1990) C3–18.
60. Nelson MT, Standen NB, Brayden JE, Worley JF, Noradrenaline contracts arteries by activating voltage-dependent calcium channels. Nature. 336 (1988) 382–385.

Figure legends

Fig. 1. Expression of MARCKS in mouse and rat mesenteric artery.

A, Representative western blot for MARCKS expression from tissue lysates of mouse and rat mesenteric arteries using an anti-MARCKS antibody. B, Immunostaining of single freshly isolated mouse and rat mesenteric artery VSMCs labelled with the same anti-MARCKS antibody as used in A. Control experiments were performed by replacing anti-MARCKS antibody with goat serum, or by omitting anti-MARCKS or donkey anti-goat antibodies. Immunoblots are representative of N=3 experimental preparations using n=3 animals per preparation, and immunocytochemical images are representative of data from n=3 animals with N≥3 cells per animal.

Fig. 2. Effects of methoxamine (MO) and MANS on contractility of mouse mesenteric artery.

A and B, Representative traces and C, mean concentration-effect curves of MO or MANS on artery segments. D, Table comparing mean EC_{50} and E_{MAX} values of MO- and MANS-induced contractions. Data from n=6 animals, with N=4 vessel segments per animal. Two-way ANOVA followed by Bonferroni Post-hoc. **P*<0.05; ****P*<0.001.

Fig. 3. Effect of MARCKS knock-down on MANS-evoked contractions in mouse mesenteric arteries.

A, Representative trace and B, mean concentration-effect curve showing attenuated effect of MANS-evoked contractions in artery segments transfected with MARCKS-targeted morpholino oligonucleotides compared with vessels pre-incubated with scrambled sequences. Data from *n*=6 animals, with N≥3 vessel segments per animal. Two-way ANOVA followed by Bonferroni Post-hoc. *****P*<0.001.

Fig. 4. Effect of MARCKS knock-down on MANS- and methoxamine (MO)-evoked contractions in mouse mesenteric arteries.

A and C, Representative traces and B and D, mean concentration-effect curves showing attenuated effect of MO- and U46619-evoked contractions in artery segments transfected with MARCKS-targeted morpholino oligonucleotides compared with vessels pre-incubated with scrambled sequences. Data from *n*=6 animals, with N≥3 vessel segments per animal. Two-way ANOVA followed by Bonferroni Post-hoc. *****P*<0.001.

Fig. 5. Effect of L-type and T-type VGCC blockers on mouse mesenteric arteries pre-contracted with MANS.

A and C, Representative traces showing the effect of a L-type and T-type VGCC blockers on MANS pre-constricted tone respectively. B and D, Mean concentration-effect curves of L-type and T-type VGCC blockers on MANS precontracted tone respectively. Data from *n*=6 animals, with N≥3 vessel segments per animal.

Fig 6. Effect of MANS and methoxamine (MO) on GFP-PLCδ-PH signals in single rat mesenteric artery vascular smooth muscle cells.

A, Representative image from a single cell showing that in control conditions, the location of GFP-PLCδ-PH-mediated signals was predominantly expressed at the plasma membrane. In the same cell, application of MANS had no significant effect on PLCδ-PH-mediated signals while subsequent treatment with MO induced translocation of signals to the cytosol. B, Line scans showing GFP-PLCδ-PH signals across the cell width in control conditions, following treatment with MANS and subsequent application of MO. Mean data showing GFP-PLCδ-PH Fm:Fc ratios (C) and % surface fluorescence (D) in control conditions, treatment with MANS, followed by application of MO. Data from *n*=6 animals, with N≥4 cells per animal. Paired students *t*-test. ****P<0.001. ns indicates not significant.

Fig 7. Effect of MANS and MO on membrane potential of rat mesenteric artery VSMCs.

A and B, representative traces from two different VSMCs with resting membrane potentials of -58 mV and -54 mV respectively. MO evoked concentration-dependent depolarisations between 1-100 μM whereas MANS induced a membrane depolarisation only at 100 μM. C, Mean data of the effect of MO and MANS membrane potential. Data from N=at least 6 patches from *n*=3 animals.

Fig. 8. Cellular distribution of MARCKS and CaV1.2 in mouse mesenteric artery VSMCs.

A and B, Representative images and mean data showing in that MARCKS (green) and CaV1.2 (red) co-localised at the plasma membrane of control VSMCs. Pre-treatment of two different VSMCs with either MANS or MO caused translocation of MARCKS to the cytosol whilst CaV1.2 remained at the plasma membrane. Data from *n*=3 animals, with N≥6 cells per animal. One-way ANOVA. ns indicates not significant. ****P<0.001.

Fig. 9. Interactions between PIP_2 and MARCKS, and PIP_2 and CaV1.2 in tissue lysates from rat mesenteric arteries.

A, Representative dot-blot with an anti-PIP_2 antibody after immunoprecipitation (IP) with either anti-MARCKS (top panels) or anti-CaV1.2 antibodies (bottom panels) from vessel segments pre-treated with distilled water (control), MANS, and MO. B and C, Mean data showing the effect of MANS or MO on PIP_2 + MARCKS and PIP_2 + CaV1.2 interactions. Data from N=3 experimental preparations with *n*=3 animals used per preparation. One-way ANOVA. *P<0.05, **P<0.01.

Fig. 10. Effect of MANS on whole-cell VGCC activity in single rat mesenteric artery VSMCs.

A, Representative traces showing that control whole-cell VGCC currents (black) from freshly isolated rat mesenteric artery VSMCs were significantly increased at -50 mV and -10 mV but reduced at +20 mV following bath application of MANS (red) and that VGCC currents were subsequently blocked by nicardipine (green). B, Mean current-voltage (I/V) relationship of VGCC currents showing that MANS

(red) produced a significant increase in peak amplitude and a negative shift in the mean activation threshold. C and D, Representative traces and mean I/V relationship of VGCC currents showing that pre-treatment of VSMCs with wortmannin (wort) attenuated the excitatory effects of MANS (red). Data from *n*=6 animals, with N≥3 patches per animal.

Tables

None

Supplementary Information

Methods

Protein Extraction

Cell lysates were extracted from mesenteric arteries arcades of mice or rats. Vessels were weighed, placed in 3 ml/g radio immunoprecipitation assay (RIPA) lysis buffer containing protease inhibitor cocktail (PI) (Santa Cruz, USA) and cut into smaller pieces. Vessels were homogenized using a pellet pestle for 5 min and sonicated for 20 min on ice. Vessels were then centrifuged at 15,000 x *g* for 20 min at 4°C. Supernatant was carefully transferred to a new eppendorf tube and quantified by performing a protein assay. RIPA lysis buffer contained: 150 mM NaCl, 1.0% (v/v) NP-40, 1.0% (v/v) Triton X-100, 0.5% (w/v) sodium deoxycholate, 0.1% (w/v) sodium dodecyl sulfate (SDS) and 50 mM Tris (pH 8.0).

Western Blotting

One-dimensional protein gel-electrophoresis was performed in 4-12% Bis-Tris gels in a Novex mini-gel system (Invitrogen, UK). Samples were mixed with Nu-Page LDS sample buffer (Life Technologies, UK), heated for 5 min at 95°C and run alongside a protein standard. 4-12% gels were run with NuPage MOPS-SDS running buffer (Life Technologies, UK) mixed with 500 µl NuPage antioxidant (Invitrogen, UK), at 200 mV for 50 min. Separated proteins were transferred onto a PVDF membrane (Life Technologies, UK) using iBlot transfer system at 20V for 7 min (Invitrogen, UK). Membranes were then immediately blocked in 5% (w/v) milk powder in PBS + 0.05% (v/v) Tween (PBST) for 1 h on a gyro-rocker at room temperature. Membranes were then incubated in anti-MARCKS (1:200; SC-6455, Santa Cruz, USA) antibody diluted in 5% (w/v) milk/PBST overnight at 4°C on a gyro-rocker. The next morning membranes were washed 3 times for 10 min at room temperature with PBST. Membranes were then incubated with a horseradish peroxidase-conjugated antibody diluted in milk/PBST for 1 h on a gyro-rocker at room temperature. Membranes were subsequently washed 4 times for 15 min in PBST on a gyro-rocker at room temperature before being treated with electrochemiluminescence (ECL) prime western blotting detection reagent (GE Healthcare, UK) for 1 min. Immunoreactive bands were visualized using photographic films (ThermoFisher Scientific, UK).

VSMC Isolation

Mesenteric arteries from mice or rats were enzymatically dispersed into single VSMCs by incubation in 0 mM Ca^{2+}-DPSS with 0.5 mg/ml protease (Sigma, UK) for 5 min followed by incubation with 50 µM Ca^{2+}-DPSS 1 mg/mL collagenase type IA (Sigma, UK) for 14 min at 37°C. Vessels were then washed in 50 µM Ca^{2+}-DPSS for 10 min at 37°C and further incubated in 50 µM Ca^{2+}-DPSS at room temperature for 10 min. Cells were then released into the solution by gently triturating the tissue using a fire polished wide-bore Pasteur pipette. The suspension of cells was then centrifuged at 1000 x *g* for 2 min to form a loose pellet that was subsequently re-suspended in 0.75 mM Ca^{2+}-DPSS. Normal DPSS contained (mM): 126 NaCl, 6 KCl, 10 glucose, 11 HEPES, 1.2 $MgCl_2$ and 1.5 $CaCl_2$, with pH adjusted to 7.2 with 10 M NaOH. Low Ca^{2+}-DPSS (0 mM, 50 µM and 0.75 mM) had the same composition as previously described, except that 1.5 mM $CaCl_2$ was replaced by 0 mM, 50 µM and 0.75 mM $CaCl_2$, respectively.

Isometric Tension Recordings

Segments of mouse superior mesenteric artery were mounted on a wire myograph and normalised. Vessel segments were equilibrated and assessed for vessel viability followed by endothelium integrity before one of five experimental protocols were performed.

Protocol 1- To investigate the effect of MANS on vascular contractility, increasing concentrations of MANS (1 nM-100 µM) (Gene-med synthesis, USA), a synthetic selective MARCKS inhibitor, was cumulatively added to vessel segments. These responses were compared to contractions produced by increasing concentrations of methoxamine (MO) (1 nM- 100 µM) (Sigma, UK).

Protocol 2-To examine whether contractions produced by MANS peptide were sensitive to VGCC blockers, increasing concentrations of various VGCC blockers or equivalent dilutions of their appropriate vehicle control were cumulatively added to vessel segments pre-contracted with 100 µM MANS.

Protocol 3-To determine whether contractions produced by MANS were sustainable, artery segments were contracted with 100 µM MANS for at least 30 min. These contractions were compared to contractions produced by 10 µM MO.

Protocol 4-To explore whether contractions produced by MANS were reproducible with multiple additions, artery segments were contracted with 100 µM MANS for at least 5 min. MANS was then washed out and artery segments were allowed to equilibrate for 10 min. Vessel segments were then subjected to a second contraction with 100 µM MANS. Artery segments were contracted three times in total and contractions produced by 100 µM MANS were compared to contractions by 10 µM MO.

Transfection of PIP_2 Biosensors

Electroporation was performed using Nucleofector™ Technology (Lonza, USA). Rat mesenteric artery branches were enzymatically dispersed into single VSMCs and counted using a Countess® automated cell counter (Invitrogen, UK). Next, $1x10^6$ cells were centrifuged at 100 x *g* for 10 min at room temperature. Cells were then re-suspended in 100 µl room temperature basic nucleofector kit primary smooth muscle cell solution (Lonza, USA) and combined with 2 µg plasmid DNA (GFP-PLCδ-PH or GFP-Tubby). Cell/DNA suspension was transferred into a supplied cuvette and the appropriate nucelofector programme (U-025) was selected. Following electroporation, 500 µl pre-warmed cell culture media was immediately added to the cell/DNA suspension. Samples were then seeded on a 96 well plate overnight at 37°C in 95% O_2 and 5% CO_2 in a humidified incubator. The following morning, cell culture media was replaced (with fresh cell culture media) and cells were incubated at 37°C in 95% O_2 and 5% CO_2 in a humidified incubator for a further 24 h before being imaged.

Immunoprecipitation

Immunoprecipitation was carried out using the Millipore Catch and Release kit (MERCK, UK), where spin columns were loaded with 500 µg of cell lysate protein and 4 µg of anti-MARCKS (1:100; SC-6455, Santa Cruz, USA) or anti-CaV1.2 (1:100; ACC-003, Alomone, Israel) primary antibody for 1 h at room temperature. Non-precipitated proteins were washed away with Millipore Catch and Release wash buffer and immunoprecipitated samples were then eluted with Millipore Catch and Release non-denaturing elution buffer. Immunoprecipitated samples were subsequently used for dot-blotting.

Proximity Ligation Assays

Interactions between MARCKS and CaV1.2 were studied with Duolink® In Situ Red Starter Kit (Sigma, UK). Freshly dispersed mouse mesenteric VSMCs (unstimulated or pre-treated with various agonists or their vehicle controls) were placed on polylysine coated microscope slides and left to adhere for 1 h at room temperature before being fixed with 4% (w/v) PFA for 15 min. Cells were then rinsed with ice cold PBS twice for 10 min and permeabilized with PBS containing 0.10% (v/v) Triton X-100 for 10 min at room temperature. Cells were then washed with ice cold PBS, 3 times every 5 min, and incubated with Duolink blocking buffer for 1 h at 37°C. Cells were then incubated with anti-MARCKS (1:50; SC-6455, Santa Cruz, USA) and anti-CaV1.2 (1:50; ACC-003, Alomone, Israel) antibodies, diluted in Duolink antibody diluent solution, overnight at 4°C. The following morning cells were washed with ice cold PBS, twice for 5 min, and incubated with oligonucleotide conjugated secondary antibodies, diluted in Duolink antibody diluent solution (1:5), for 1 h at 37°C. Unbound secondary antibodies were removed by washing with Wash Buffer A twice for 2 min and cells were incubated in Ligation-Ligase Solution for 1 h at 37°C. Cells were then washed with Wash Buffer A twice for 2 min and incubated in Amplification-Polymerase Solution for 2 h at 37°C in the dark. Then cells were washed with Wash Buffer B twice for 10 min and 0.01x Wash Buffer B for 1 min and slides

were left to dry at room temperature in the dark. Next, cells were treated with Duolink *In Situ* Mounting Medium with DAPI and cover slips were mounted to microscope slides. Cells were imaged using a Zeiss LSM 510 laser scanning confocal microscope (Carl Zeiss, Germany). Excitation was produced by 594 nm lasers and delivered to cells *via* a Zeiss Apochromat x63oil-immersion objective (numerical aperture, 1.4). Fluorescent puncta were captured using LSM 510 software (release 3.2; Carl Zeiss, Germany). The mean number of puncta per cell was calculated by counting the number of particles across a z-stack of the cell. Final images were produced using PowerPoint (Microsoft, USA). Control experiments were carried out by omitting both primary antibodies.

IP_3 ELISA

IP_3 levels were determined with a mouse IP_3 ELISA kit (BlueGene Biotech, China) following the manufacturer's instructions. Mouse mesenteric arteries were dissected, divided into three, and treated with vehicle, 100 μM MANS peptide, or 10 μM MO before being lysed as previously described. 100 μl standards or samples (in triplicate) were added to the appropriate wells. Next, 10 μl balance solution was added into 100 μl samples. Then 50 μl of conjugate was added to each well and the plate was incubated for 1 h at 37°C in the dark. The plate was then washed five times with 1 x wash buffer to remove unbound antibodies before being inverted and blot dried. Next, 50 μl substrate A and 50 μl substrate B were added to each well, sequentially, and the plate was incubated for 30 min at 37°C in the dark. Finally, 50 μl stop solution was added to each well and the absorbance reading at 450nm was determined using a microplate reader (SpectraMax 340PC384; Molecular Devices, USA).

Figure legends

Fig. S1. Characterisation of MANS-evoked contractions in mouse superior mesenteric artery segments.

A, Representative traces and mean data comparing sustainability of contractions induced by MO (left panel) and MANS (right panel). B, Representative traces and mean data comparing the reproducibility of contractions induced by MO (left panel) and MANS (right panel) with multiple additions. Data from *n*=3 animals, with N≥3 vessel segments per animal.

Fig. S2. Morpholino-induced MARCKS knock-down in mouse mesenteric artery tissue lysates.

A, Representative images showing increased fluorescence of artery segments transfected with fluorescein-tagged morpholino (right panel) compared with artery segments transfected with non-fluorescein-tagged morpholino (left panel). Representative western blots (B and C), and mean data comparing protein expression of MARCKS (D), α-tubulin (E) total protein (F), in tissue lysate from vessel segments pre-treated with scrambled or MARCKS-targeted morpholino. Data from N=6 experimental preparations with *n*=2 animals used for each preparation. Unpaired students *t*-test. **P*<0.05. ns indicates not significant.

Fig. S3. Morpholino-induced MARCKS knock-down on CaV1.2 levels in mouse mesenteric artery tissue lysates.

A and B, Representative western blot and mean data showing protein expression of CaV1.2 in tissue lysate from vessel segments pre-treated with scrambled or MARCKS-targeted morpholino. Data from N=6 experimental preparations with *n*=2 animals used for each preparation. Unpaired students *t*-test. **P*<0.05. ns indicates not significant.

Fig. S4. Expression and localisation of MARCKS and CaV1.2 in single mouse mesenteric VSMCs following MARCKS knock-down.

A, Representative images of scrambled (top panel) or MARCKS-targeted (bottom panel) morpholino pre-treated VSMCs co-immunolabelled with anti-MARCKS (green) and anti-CaV1.2 (red) antibodies. B and C, Representative and mean data of line scans showing anti-MARCKS (left panel) and anti-CaV1.2 (right panel) signals across the cell width and graphs showing fluorescent intensities at the cell surface in scrambled and MARCKS-targeted morpholino pre-treated VSMCs. Data from *n*=4 animals with N≥6 cells per animal. Unpaired students *t*-test. *****P*<0.0001. ns indicates not significant.

Fig. S5. Effect of MARCKS knock-down on resting tension and evoked contractions.

Tables showing mean data comparing resting tension (A), and MANS- (B), methoxamine (MO)- (C) and U46619-evoked contractions (D) in scrambled and MARCKS-targeted morpholino treated vessels. Data from *n*=6 animals, with N=4 segments per animal. Two-way ANOVA. *****P*<0.0001.

Fig. S6. Effect of MARCKS knock-down on KCl-and ionomycin-induced contractions in mouse mesenteric arteries.

A and B, Representative traces and mean data comparing contractions induced by KCl (top panel) and ionomycin (bottom panel) in scrambled and MARCKS-targeted morpholino oligonucleotides treated vessels. Data from *n*=4 animals, with N≥4 segments per animal.

Fig. S7. Table comparing the mean data of L-type and T-type VGCC blockers on MANS pre-constricted tone in mouse mesenteric artery segments.

Fig 8. Effect of MANS and methoxamine (MO) on GFP-tubby signals in single rat mesenteric artery vascular smooth muscle cells.

A, Representative image from a single cell showing that in control conditions, the location of GFP-tubby-mediated signals was predominantly expressed at the plasma membrane. In the same cell, application of MANS had no significant effect on GFP-tubby-mediated signals while subsequent treatment with MO induced translocation of signals to the cytosol. B, Line scans showing GFP-tubby signals across the cell width in control conditions, following treatment with MANS and subsequent

application of MO. C, Mean data showing GFP-tubby Fm:Fc ratios in control conditions, treatment with MANS, followed by application of MO. Data from *n*=6 animals, with N≥4 cells per animal. Paired students *t*-test. ****P<0.001. ns indicates not significant.

Fig. S9. Comparison of IP_3 levels in mouse mesenteric artery tissue lysates from vessel segments pre-treated with MANS or methoxamine (MO).

Mean data showing that pre-treating vessel segments with MANS had no significant (ns) effect on relative IP_3 levels in tissue lysate. Whereas, pre-treating segments with MO increased relative IP_3 levels in tissue lysate. Data from N=3 experimental preparations with *n*=3 animals used per preparation. One-way ANOVA. ****P<0.0001. ns indicates not significant.

Fig. S10. Interaction between MARCKS and CaV1.2 in single mouse mesenteric artery VSMCs.

Representative proximity ligation assay (PLA) images of single VSMCs (A) and mean data (B) which show that in control cells MARCKS and CaV1.2 interact at the plasma membrane. Pre-treatment with MANS or methoxamine (MO) reduced interactions between MARCKS and CaV1.2. Data from *n*=6 animals, with N=≥6 cells per animal. One-way ANOVA. ****P<0.0001.

Fig. S11. Effect of wortmannin on PIP_2 levels in VSMCs.

A, Representative images of a single GFP-tubby transfected rat mesenteric artery VSMC, line scan, and mean data showing that wortmannin (Wort) reduced GFP-tubby signals at the plasma membrane and caused translocation of GFP-tubby signals to the cytosol. Data from *n*=4 animals, with N≥4 cells per animals. B, Representative image of a single GFP-PLCδ-PH transfected rat mesenteric artery VSMC, line scan, and mean data showing that wortmannin reduced GFP-PLCδ-PH- signals at the plasma membrane. Data from *n*=4 animals, with N≥4 cells per animal. C, Representative dot-blot with an anti-PIP_2 antibody which shows that wortmannin reduced PIP_2 fluorescence intensity (top panel) and that immunoprecipitation with a non-specific IgG or blotting with lysis or elution buffer (bottom panel) produced no fluorescence. Data from N=3 preparations with *n*=3 animals used per preparation. Paired students *t*-test. ***P<0.001; ****P<0.0001.

Figure S12. Proposed signalling pathway coupling Gq-receptor stimulation and MARCKS to regulation of vascular contractility.

The present work indicates that MARCKS regulates vascular contractility by modulating voltage-gated Ca^{2+} channel (VGCC) activity. We propose that in resting, unstimulated vascular smooth muscle cells (VSMCs), MARCKS associates with VGCCs to inhibit contractility by sequestering local PIP_2 levels, reducing PIP_2-mediated facilitation of VGCC activity. Disinhibition of MARCKS (represented by the red lines) by MANS or stimulation of Gq-coupled receptors by vasoconstrictors (e.g. MO and U46619) leads to dissociation of MARCKS-VGCC interaction and translocation of

MARCKS to the cytosol which causes release of this sequestered PIP_2 at the plasma membrane that binds to, and facilitates VGCC activity, to promote vasoconstriction. The pathway linking Gq-coupled receptors to MARCKS is unknown but is likely to involve protein kinase C (PKC) and/or calmodulin (CaM).

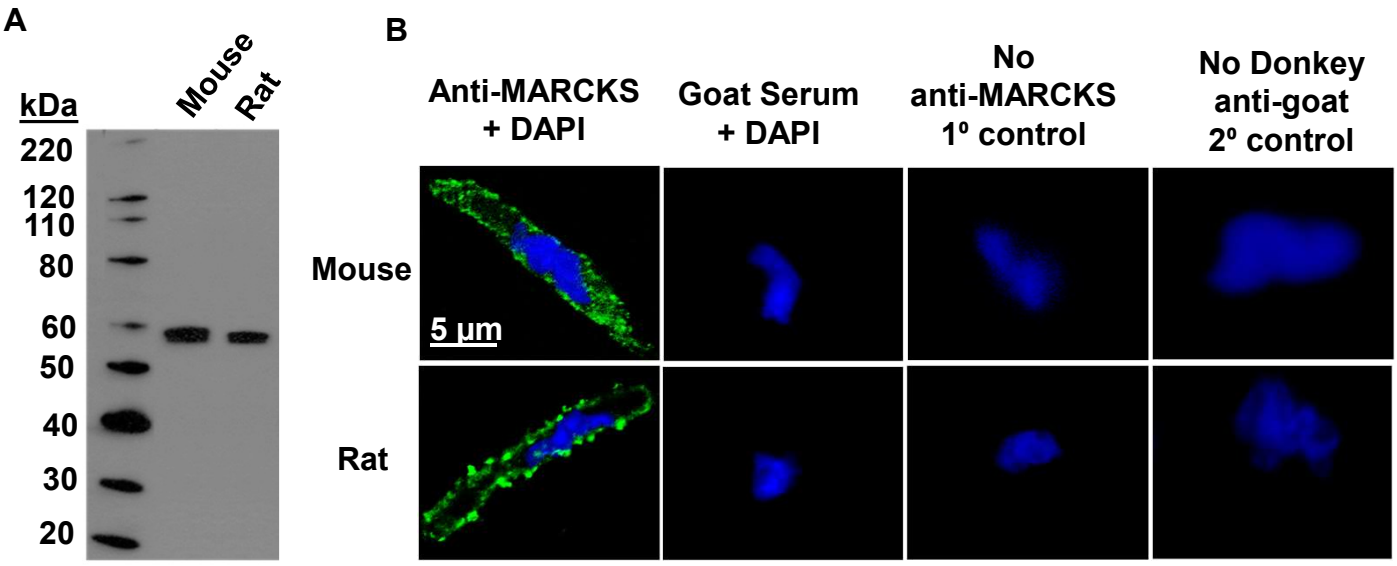
A
kDa
Mouse
Rat
220
120
110
80
60
50
40
30
20
B
Anti-MARCKS + DAPI
Goat Serum + DAPI
No anti-MARCKS 1º control
No Donkey anti-goat 2º control
Mouse
Rat
5 µm

Fig. 1

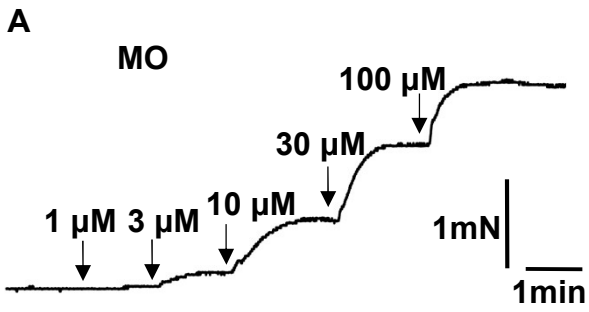

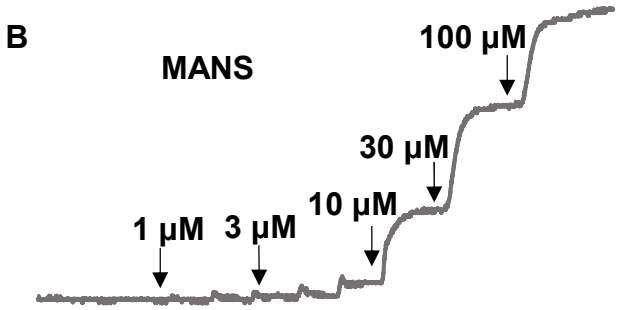

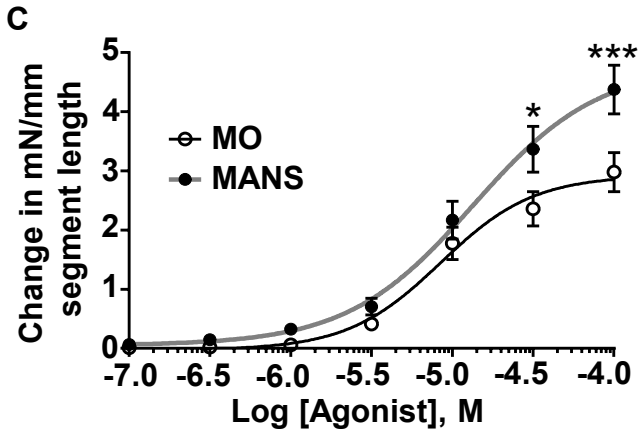

D

Agent	EC_{50}	E_{MAX}	n	N
MO	6 ± 1 µM	3 ± 0.5 mN	6	24
MANS	12 ± 2 µM	4 ± 0.5 mN	6	24

Fig. 2

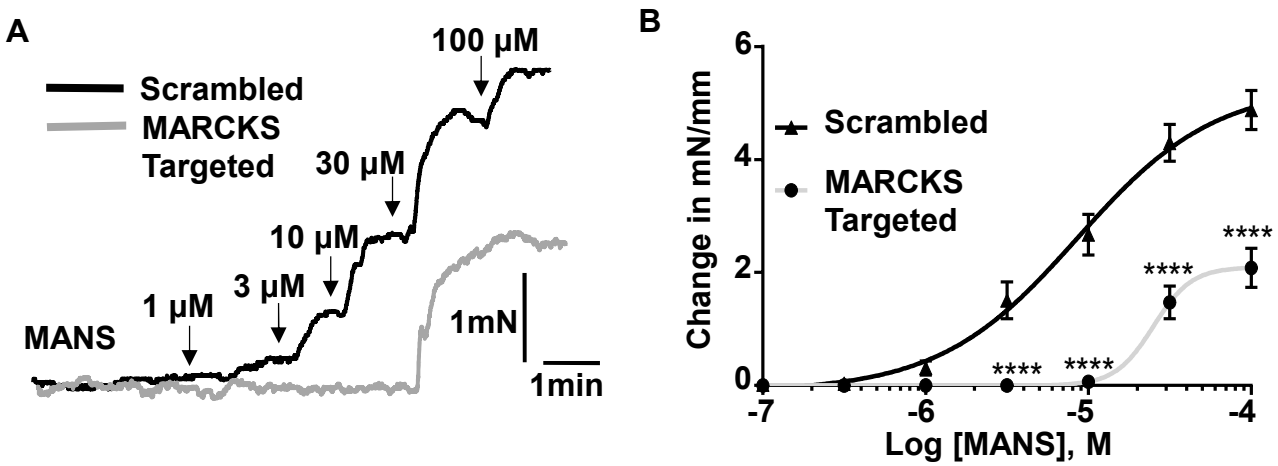
A
Scrambled
MARCKS
Targeted
MANS
1 μM
3 μM
10 μM
30 μM
100 μM
1mN
1min
B
Change in mN/mm
Scrambled
MARCKS
Targeted
****
****
****
Log [MANS], M
-7
-6
-5
-4
0
2
4
6

Fig. 3

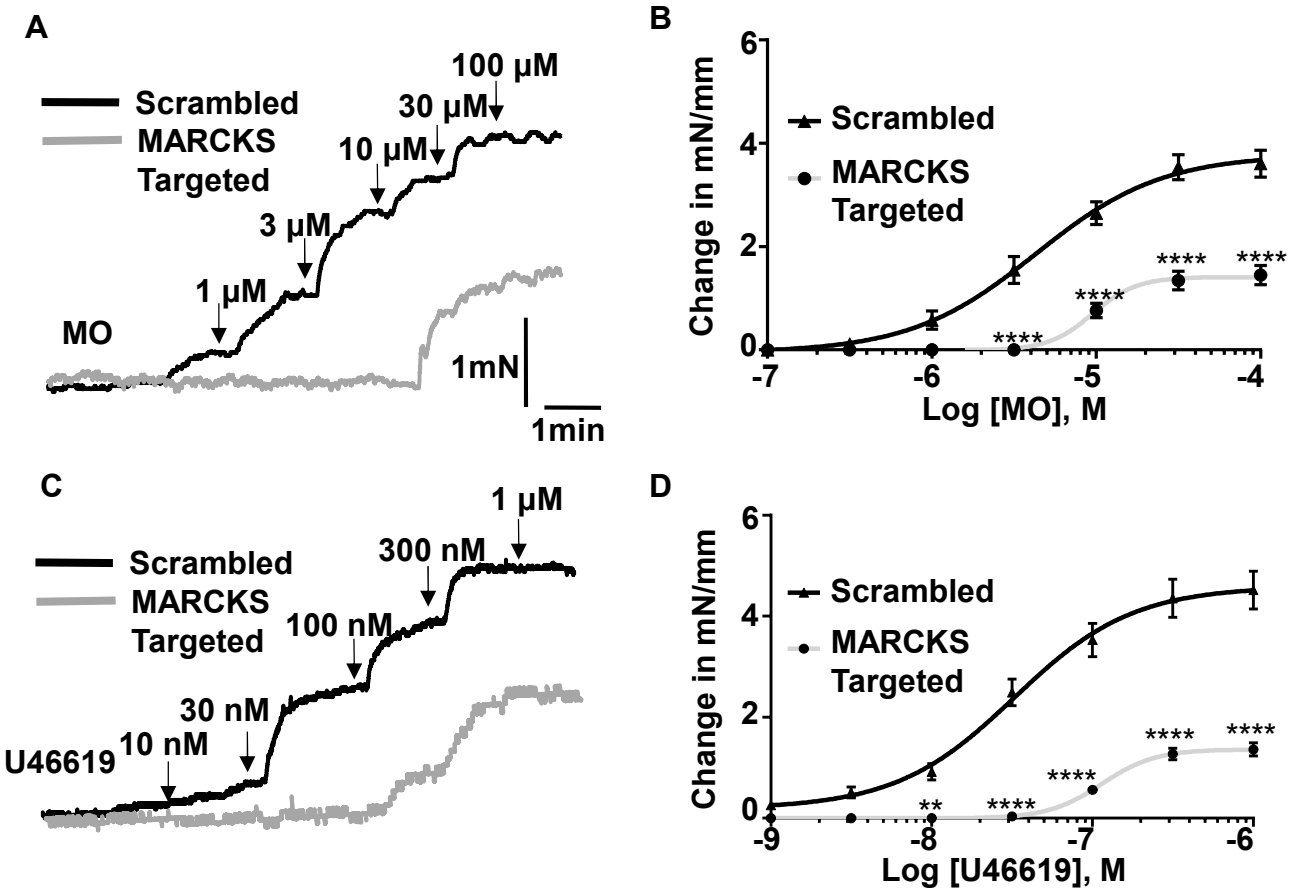
A
Scrambled
MARCKS Targeted
100 μM
30 μM
10 μM
3 μM
1 μM
MO
1mN
1min
B
Change in mN/mm
Scrambled
MARCKS Targeted
Log [MO], M
C
Scrambled
MARCKS Targeted
1 μM
300 nM
100 nM
30 nM
10 nM
U46619
D
Change in mN/mm
Scrambled
MARCKS Targeted
Log [U46619], M

Fig. 4

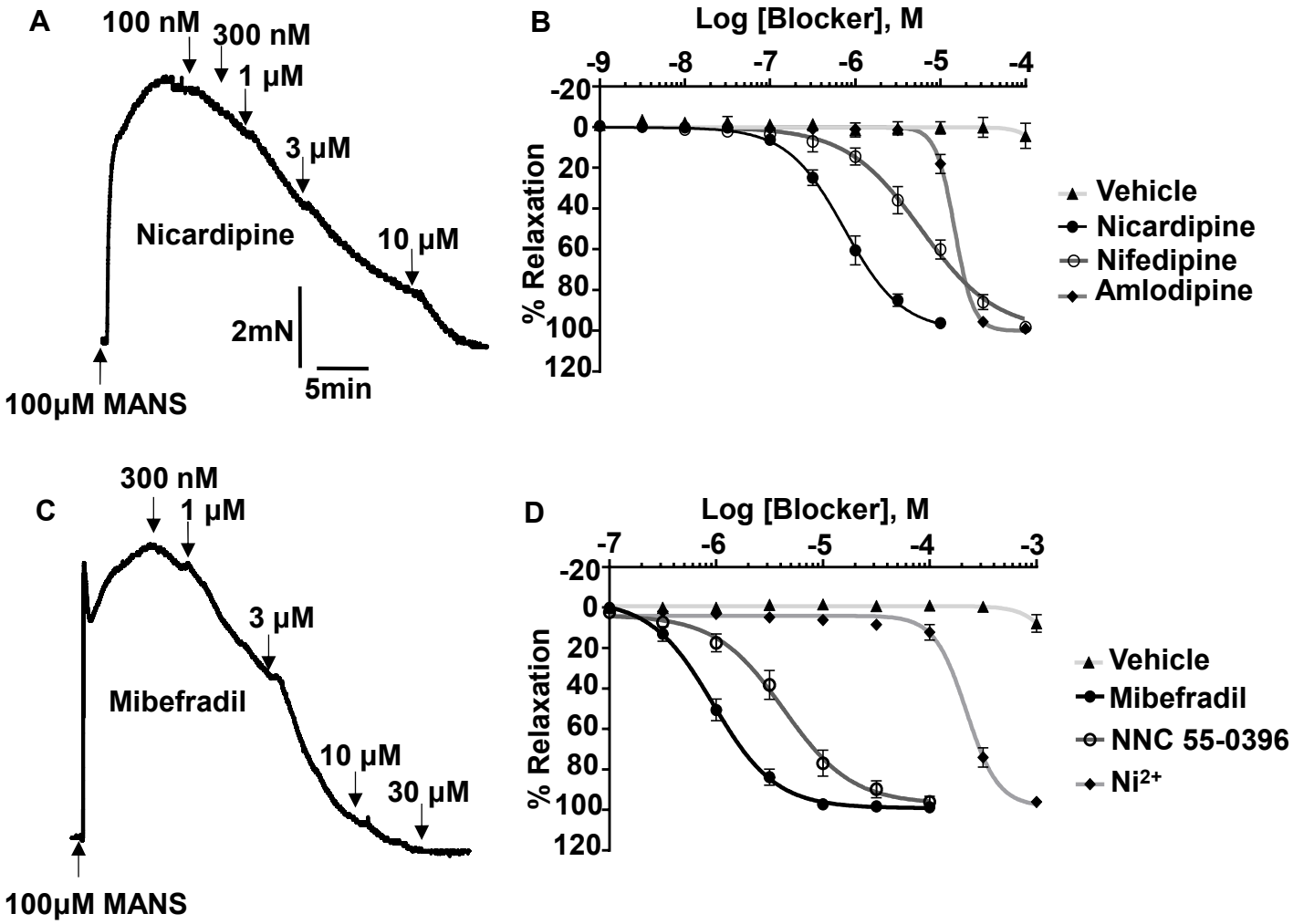
A
100 nM
300 nM
1 μM
3 μM
Nicardipine
10 μM
2mN
5min
100μM MANS
B
Log [Blocker], M
-9
-8
-7
-6
-5
-4
-20
0
20
40
60
80
100
120
% Relaxation
Vehicle
Nicardipine
Nifedipine
Amlodipine
C
300 nM
1 μM
3 μM
Mibefradil
10 μM
30 μM
100μM MANS
D
Log [Blocker], M
-7
-6
-5
-4
-3
-20
0
20
40
60
80
100
120
% Relaxation
Vehicle
Mibefradil
NNC 55-0396
Ni2+

Fig. 5

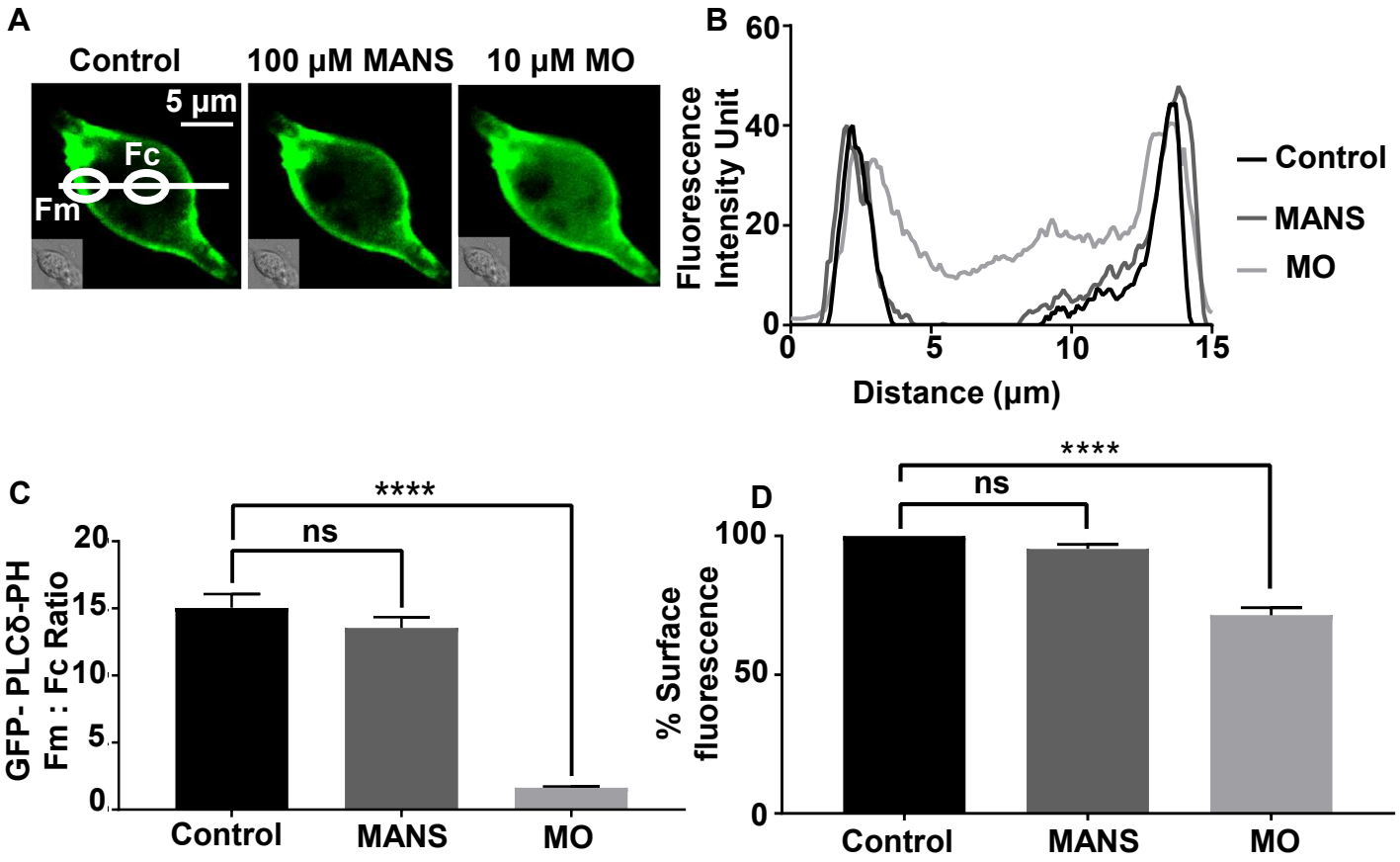
A
Control
100 µM MANS
10 µM MO
5 µm
Fc
Fm
B
Fluorescence Intensity Unit
60
40
20
0
0
5
10
15
Distance (µm)
Control
MANS
MO
C
GFP- PLCδ-PH Fm : Fc Ratio
20
15
10
5
0
****
ns
Control
MANS
MO
D
% Surface fluorescence
100
50
0
****
ns
Control
MANS
MO

Fig. 6

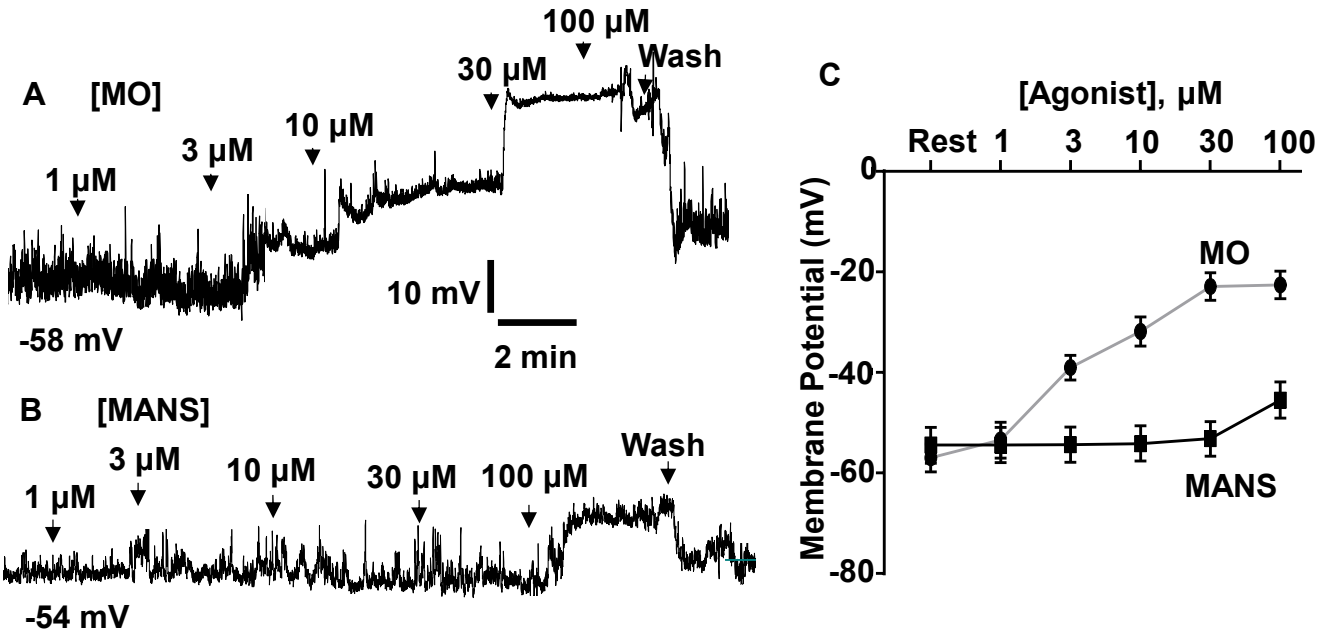
A [MO]
1 μM
3 μM
10 μM
30 μM
100 μM
Wash
10 mV
2 min
-58 mV
B [MANS]
1 μM
3 μM
10 μM
30 μM
100 μM
Wash
-54 mV
C
[Agonist], μM
Rest 1 3 10 30 100
0
-20
-40
-60
-80
Membrane Potential (mV)
MO
MANS

Fig. 7

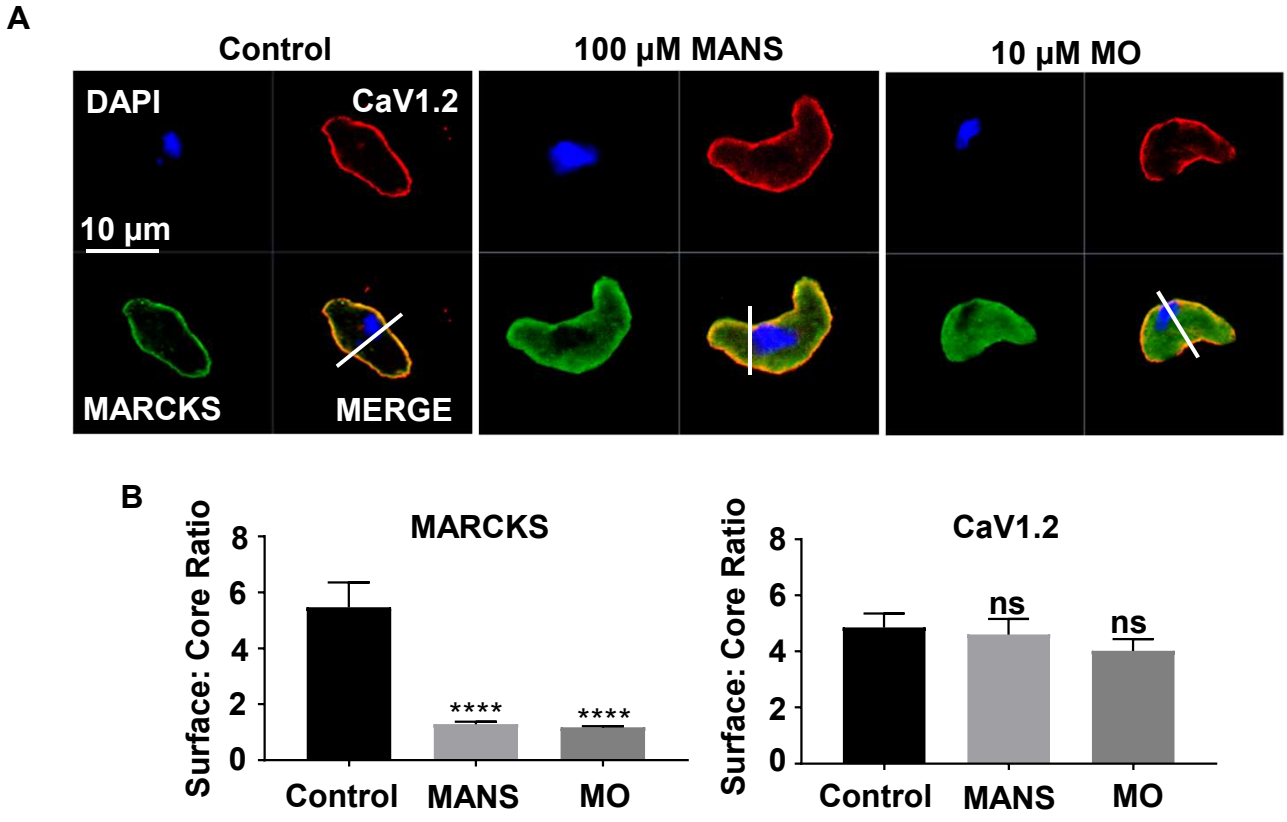
A
Control
100 µM MANS
10 µM MO
DAPI
CaV1.2
10 µm
MARCKS
MERGE
B
MARCKS
Surface: Core Ratio
8
6
4
2
0
****
****
Control
MANS
MO
CaV1.2
Surface: Core Ratio
8
6
4
2
0
ns
ns
Control
MANS
MO

Fig. 8

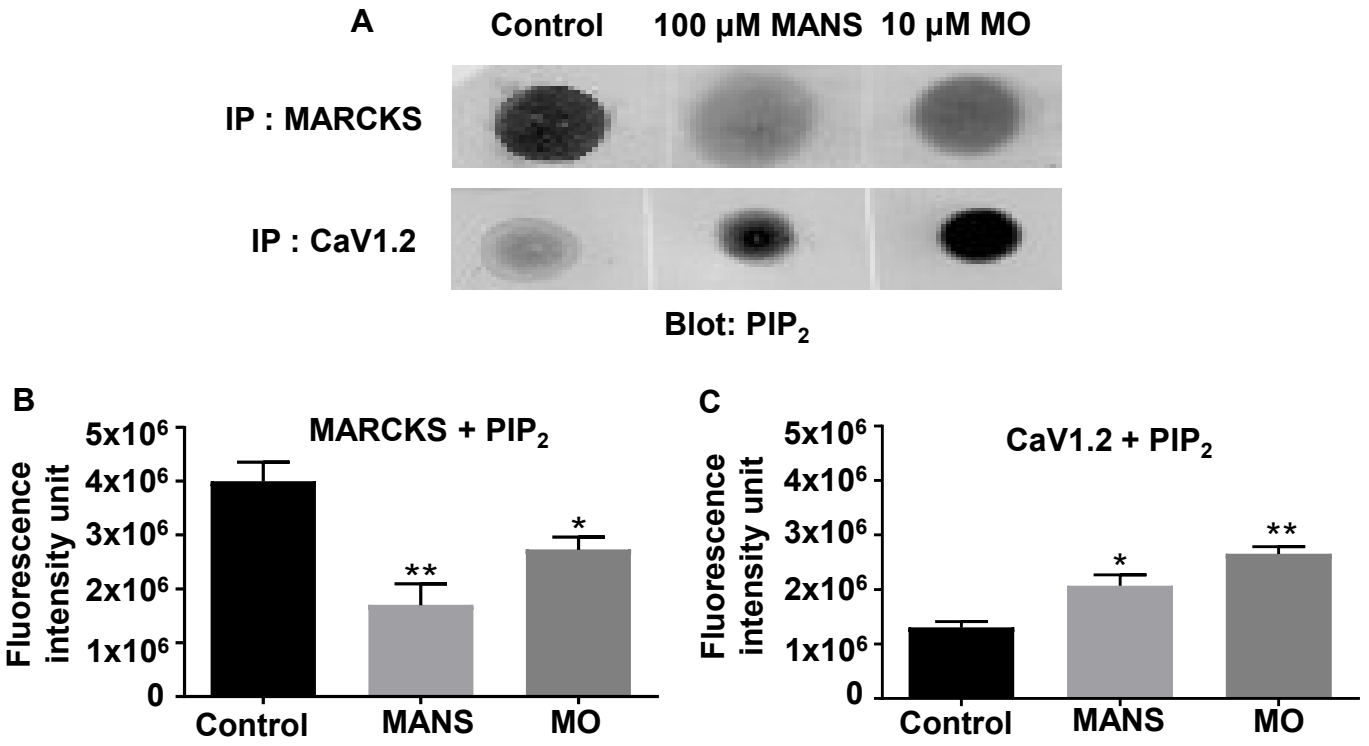
A
Control
100 μM MANS
10 μM MO
IP : MARCKS
IP : CaV1.2
Blot: PIP2
B
MARCKS + PIP2
Fluorescence intensity unit
5x10^6
4x10^6
3x10^6
2x10^6
1x10^6
0
Control
MANS
MO
**
*
C
CaV1.2 + PIP2
Fluorescence intensity unit
5x10^6
4x10^6
3x10^6
2x10^6
1x10^6
0
Control
MANS
MO
*
**

Fig. 9

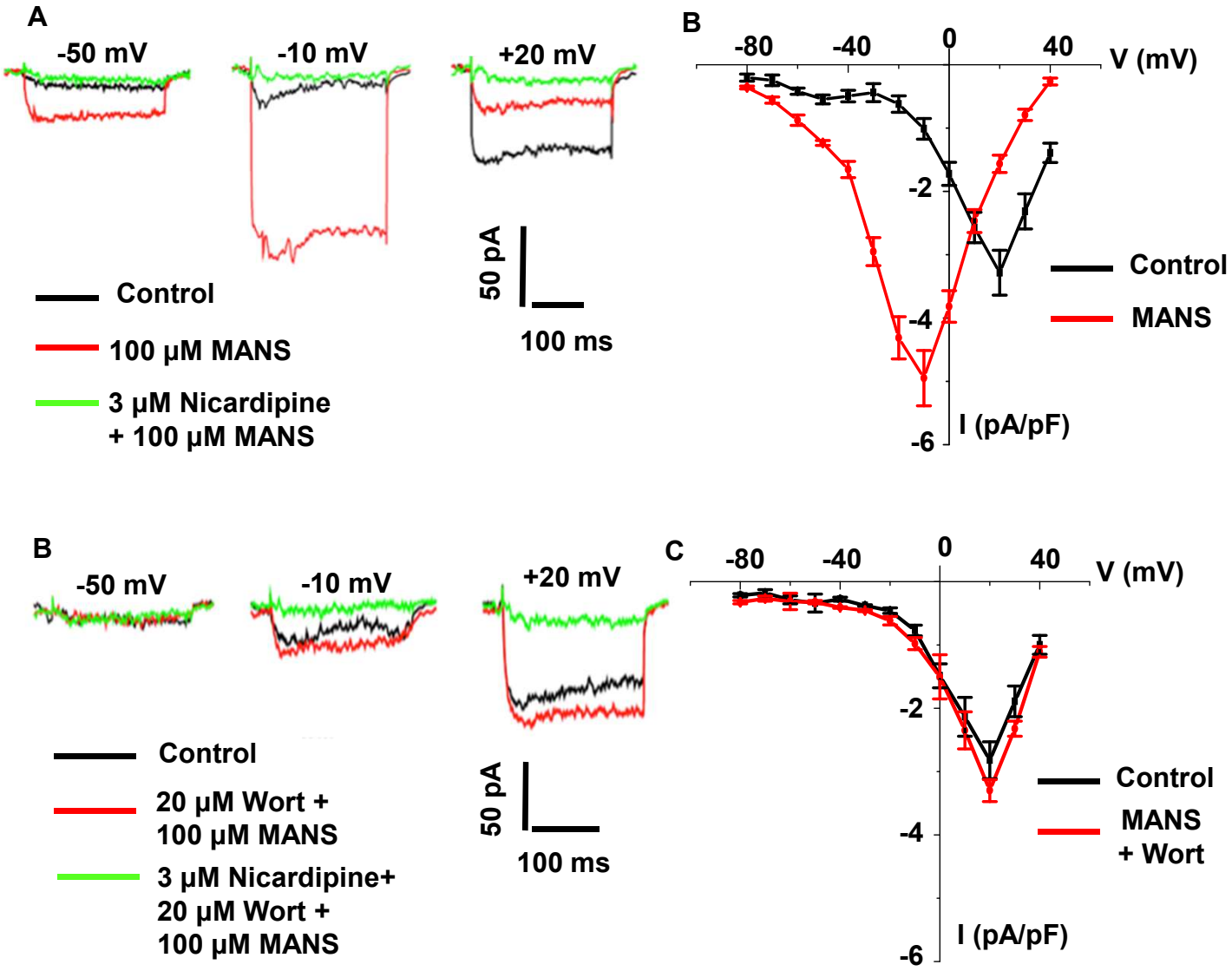
A
-50 mV
-10 mV
+20 mV
50 pA
100 ms
Control
100 µM MANS
3 µM Nicardipine
+ 100 µM MANS
B
-80
-40
0
40
V (mV)
-2
-4
-6
I (pA/pF)
Control
MANS
B
-50 mV
-10 mV
+20 mV
50 pA
100 ms
Control
20 µM Wort +
100 µM MANS
3 µM Nicardipine+
20 µM Wort +
100 µM MANS
C
-80
-40
0
40
V (mV)
-2
-4
-6
I (pA/pF)
Control
MANS
+ Wort

Fig. 10

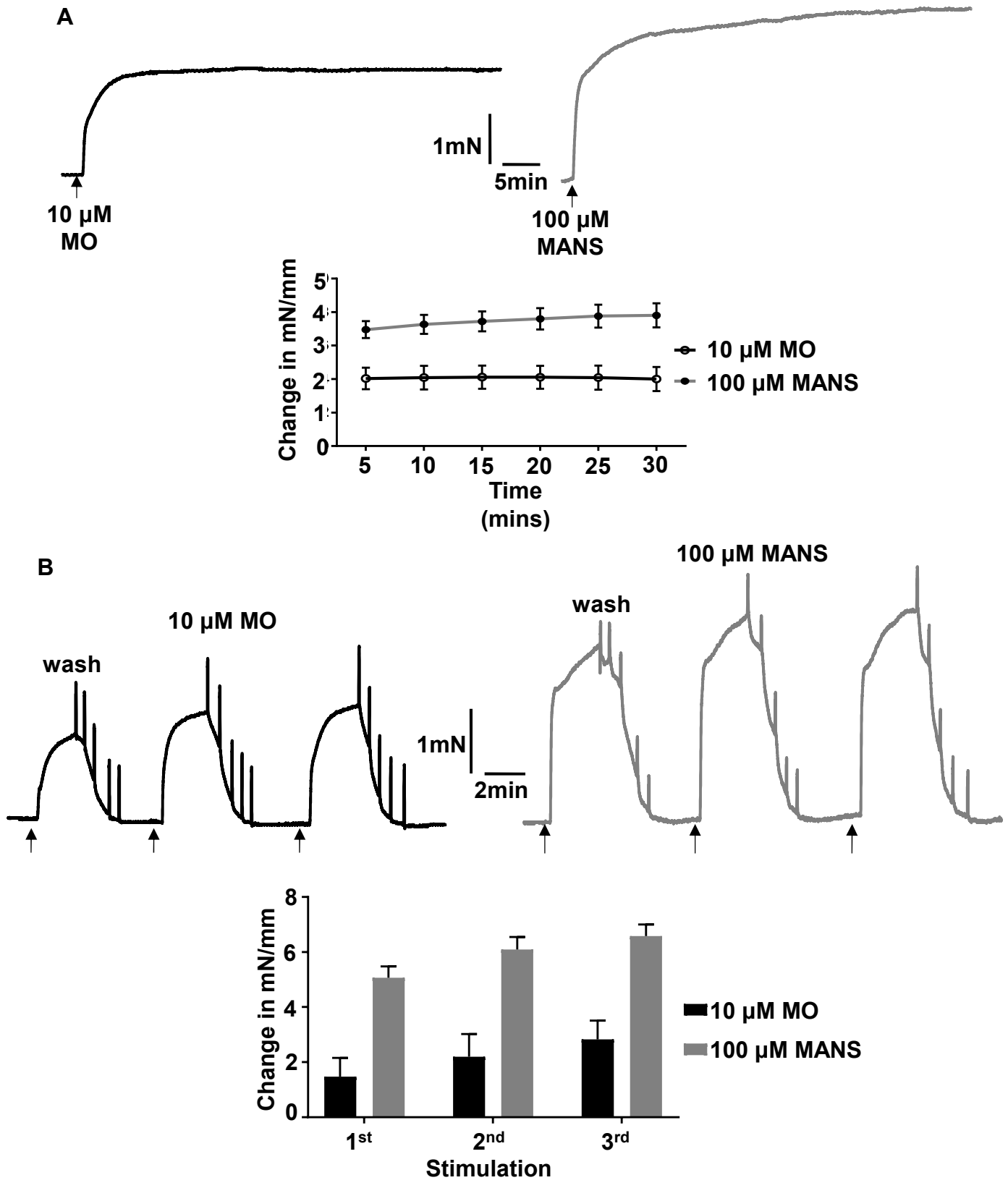
A
1mN
5min
10 µM
MO
100 µM
MANS
Change in mN/mm
Time
(mins)
10 µM MO
100 µM MANS
B
wash
10 µM MO
wash
100 µM MANS
1mN
2min
Change in mN/mm
1st
2nd
3rd
Stimulation
10 µM MO
100 µM MANS

Fig. S1

Fig. S2

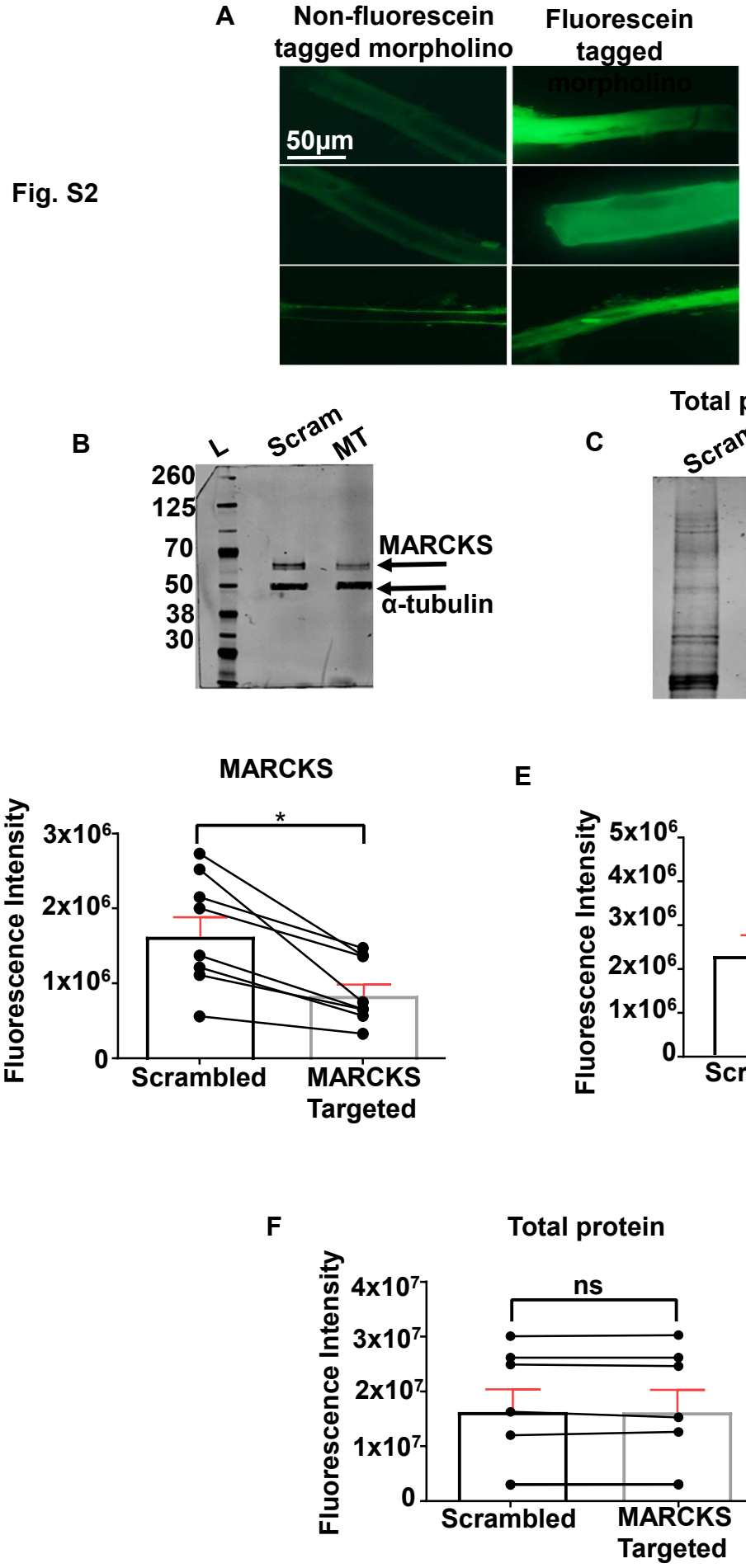
A
Non-fluorescein tagged morpholino
Fluorescein tagged morpholino
50µm
B
L
Scram
MT
260
125
70
50
38
30
MARCKS
α-tubulin
C
Total protein
Scram
MT
D
MARCKS
Fluorescence Intensity
3x10^6
2x10^6
1x10^6
0
*
Scrambled
MARCKS Targeted
E
α-tubulin
ns
Fluorescence Intensity
5x10^6
4x10^6
3x10^6
2x10^6
1x10^6
0
Scrambled
MARCKS Targeted
F
Total protein
ns
Fluorescence Intensity
4x10^7
3x10^7
2x10^7
1x10^7
0
Scrambled
MARCKS Targeted

Fig. S3

A

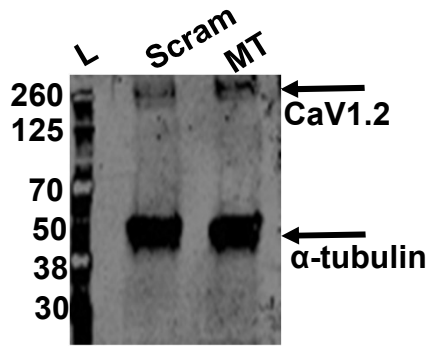
L
Scram
MT
260
125
70
50
38
30
CaV1.2
α-tubulin

B

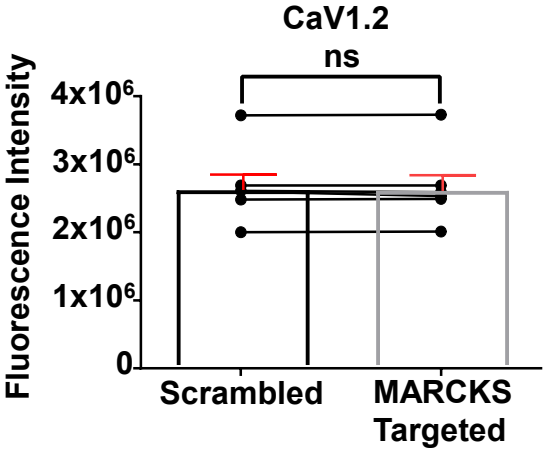
CaV1.2
ns
Fluorescence Intensity
4x10^6
3x10^6
2x10^6
1x10^6
0
Scrambled
MARCKS
Targeted

Fig. S4

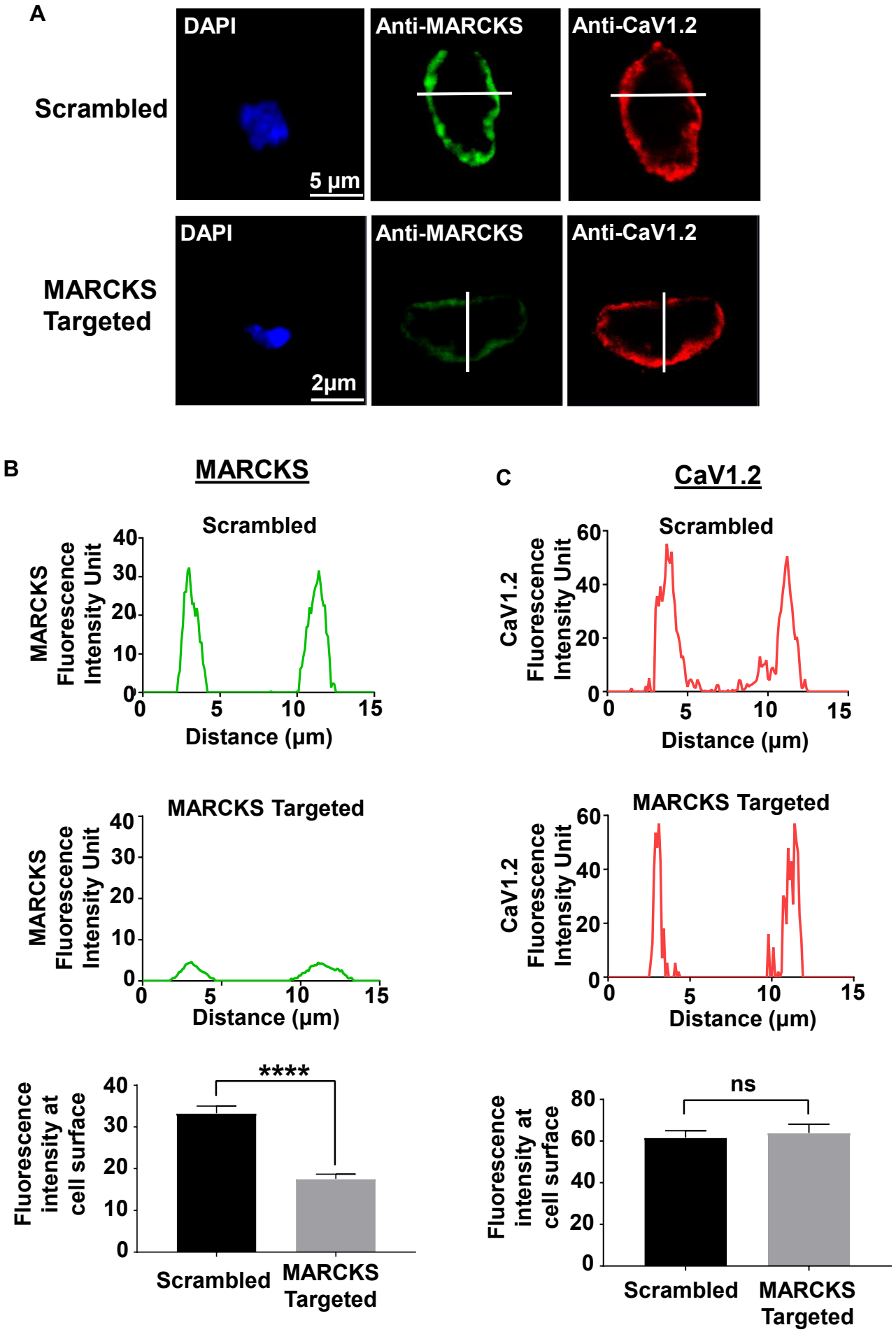
A
Scrambled
DAPI
Anti-MARCKS
Anti-CaV1.2
5 μm
MARCKS Targeted
DAPI
Anti-MARCKS
Anti-CaV1.2
2μm
B
MARCKS
Scrambled
MARCKS Fluorescence Intensity Unit
Distance (μm)
MARCKS Targeted
MARCKS Fluorescence Intensity Unit
Distance (μm)
Fluorescence intensity at cell surface
****
Scrambled
MARCKS Targeted
C
CaV1.2
Scrambled
CaV1.2 Fluorescence Intensity Unit
Distance (μm)
MARCKS Targeted
CaV1.2 Fluorescence Intensity Unit
Distance (μm)
Fluorescence intensity at cell surface
ns
Scrambled
MARCKS Targeted

A

	Scrambled	MARCKS Targeted
Resting Tension (mN/mm)	5.58 ± 0.15	5.43 ± 0.13

B

MANS	EC_{50}	E_{MAX}	*n*	*N*
Scrambled	10 ± 1 μM	4.8 ± 0.3 mN	6	24
MARCKS Targeted	36 ± 2 μM****	2.0 ± 0.2 mN****		

C

MO	EC_{50}	E_{MAX}	*n*	*N*
Scrambled	5 ± 1 μM	3.6 ± 0.2 mN	6	24
MARCKS Targeted	12 ± 1 μM****	1.5 ± 0.2 mN****		

D

U46619	EC_{50}	E_{MAX}	*n*	*N*
Scrambled	34 ± 2 nM	4.5 ± 0.4 mN	6	24
MARCKS Targeted	124 ± 12 nM****	1.4 ± 0.1 mN****		

Fig. S5

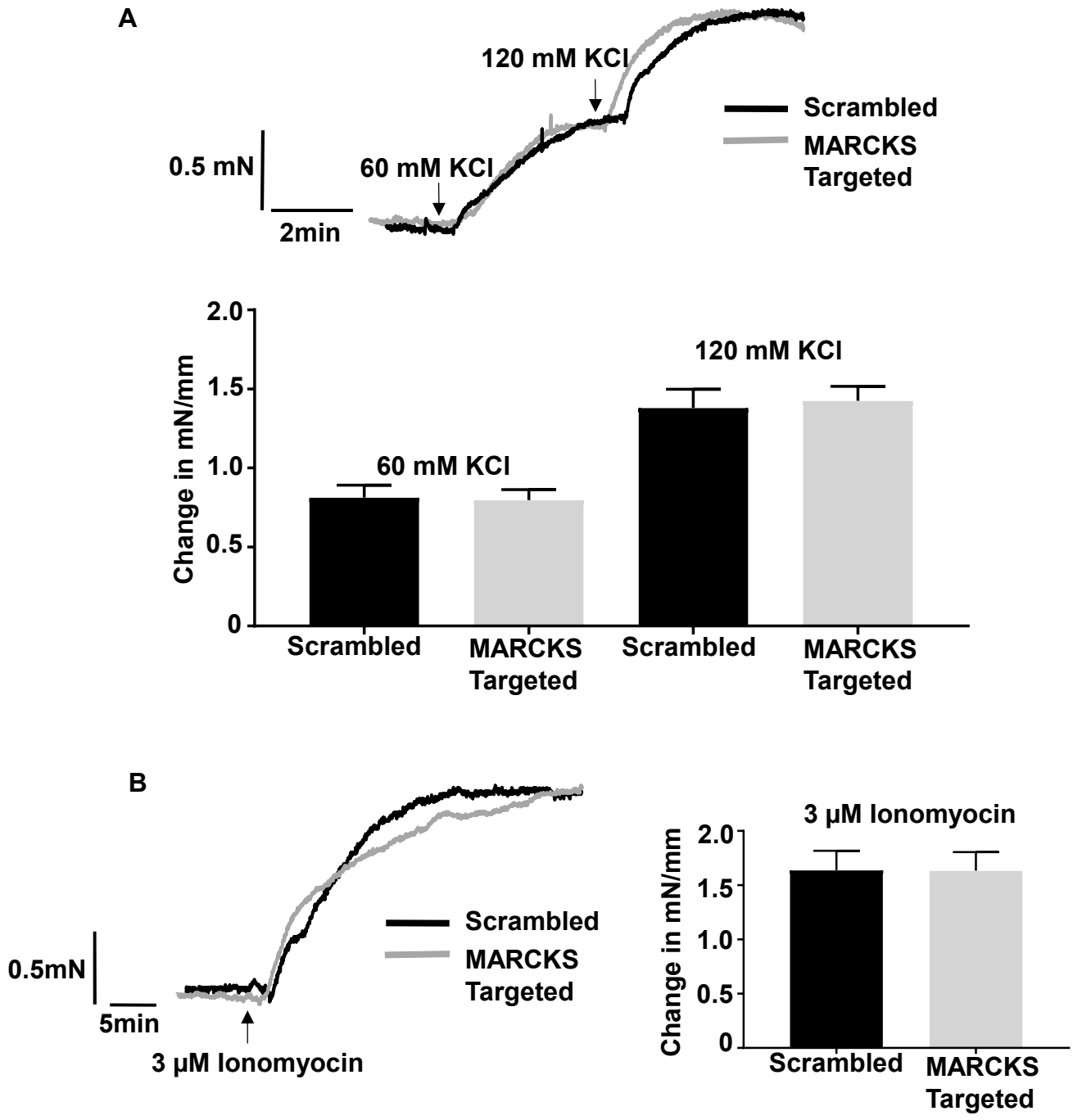
A
120 mM KCl
Scrambled
MARCKS
Targeted
0.5 mN
60 mM KCl
2min
2.0
1.5
1.0
0.5
0
Change in mN/mm
120 mM KCl
60 mM KCl
Scrambled
MARCKS
Targeted
Scrambled
MARCKS
Targeted
B
Scrambled
MARCKS
Targeted
0.5mN
5min
3 μM Ionomycin
3 μM Ionomycin
2.0
1.5
1.0
0.5
0
Change in mN/mm
Scrambled
MARCKS
Targeted

Fig. S6

Blocker	IC_{50}	IC_{100}	E_{Max} (Relaxation)	*n*	*N*
Nicardipine	1 ± 0.5 µM	2 ± 1 µM	96 ± 2 %	6	20
Nifedipine	9 ± 2 µM	17 ± 4 µM	98 ± 2 %	6	20
Amlodipine	17± 2 µM	34 ± 3 µM	99 ± 1 %	6	20
Mibefradil	1 ± 0.2 µM	2 ± 0.4 µM	99 ± 1 %	6	24
NNC 55-0396	5 ± 1 µM	9 ± 1 µM	96 ± 3 %	6	24
Ni^{2+}	250 ± 23 µM	500 ± 26 µM	99 ± 0.5 %	6	24

Fig. S7

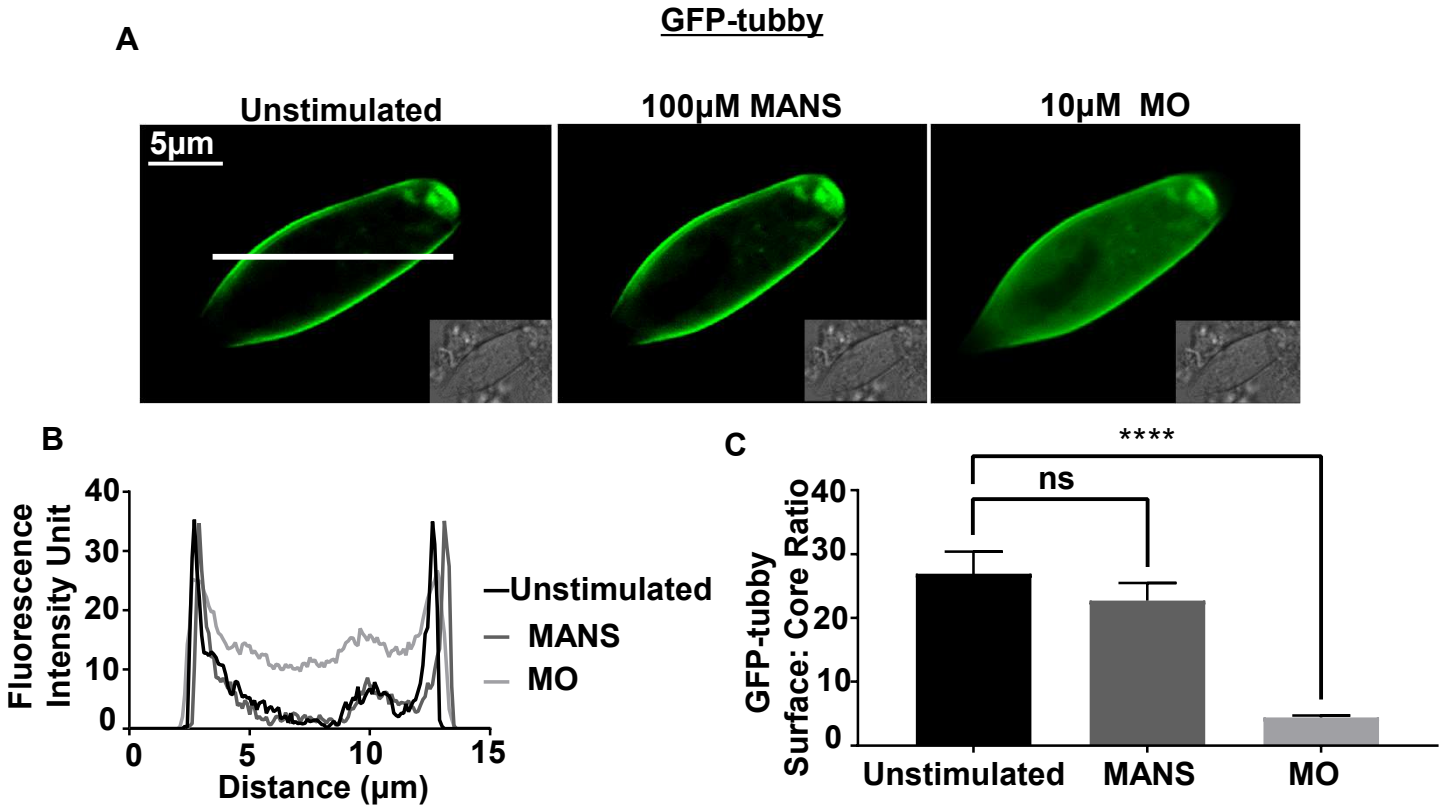
A
GFP-tubby
Unstimulated
100μM MANS
10μM MO
5μm
B
Fluorescence Intensity Unit
40
30
20
10
0
0
5
10
15
Distance (μm)
—Unstimulated
— MANS
— MO
C
****
ns
GFP-tubby Surface: Core Ratio
40
30
20
10
0
Unstimulated
MANS
MO

Fig. S8

Fig. S9

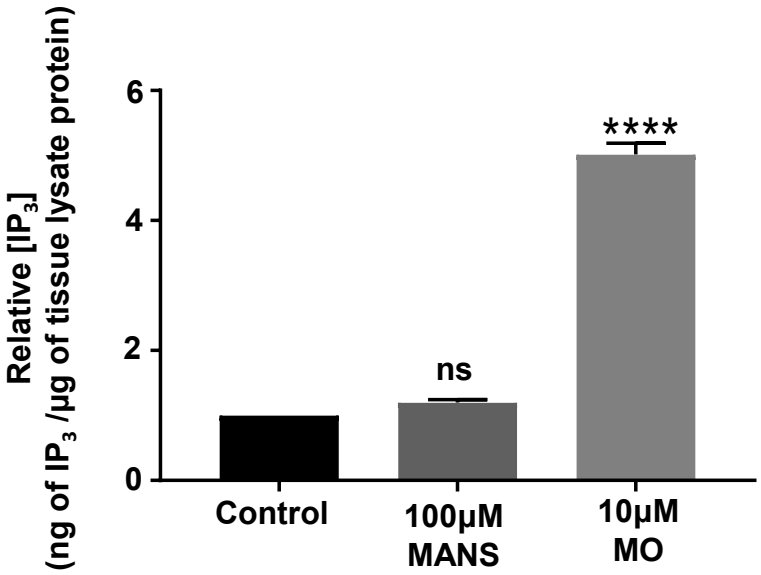
Relative [IP3]
(ng of IP3 /µg of tissue lysate protein)
6
4
2
0
ns
****
Control
100µM
MANS
10µM
MO

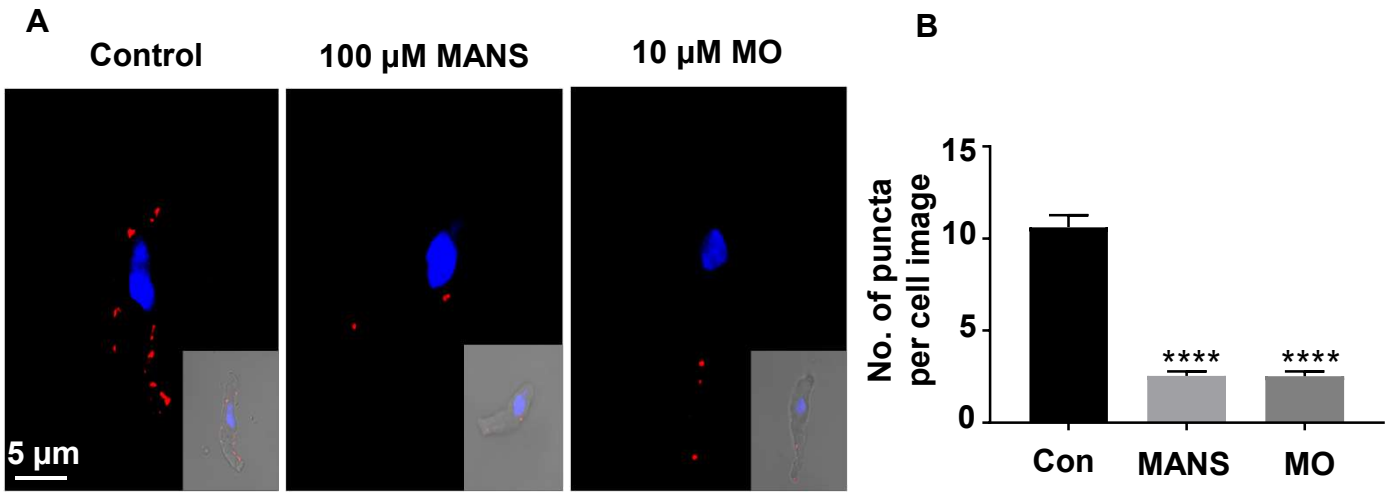
A
Control
100 μM MANS
10 μM MO
5 μm
B
No. of puncta per cell image
15
10
5
0
****
****
Con
MANS
MO

Fig. S10

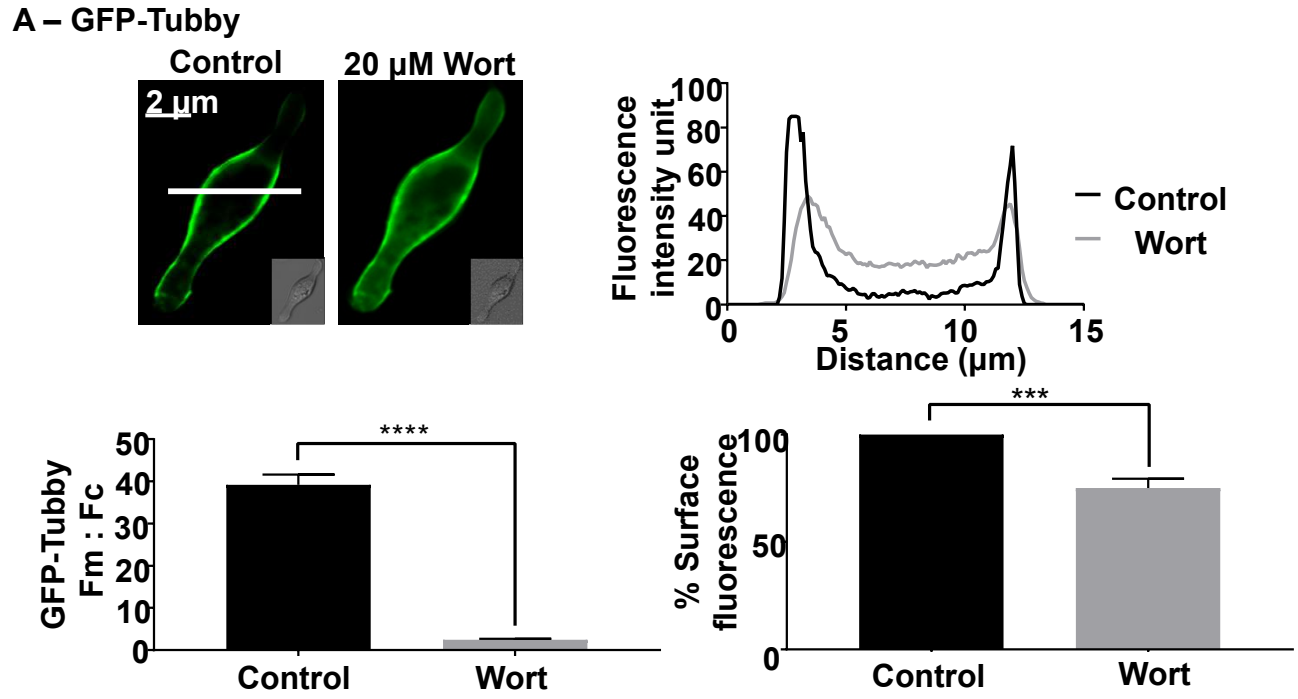
A – GFP-Tubby
Control
20 µM Wort
2 µm
Fluorescence intensity unit
Distance (µm)
Control
Wort
GFP-Tubby Fm : Fc
****
% Surface fluorescence
***
Control
Wort

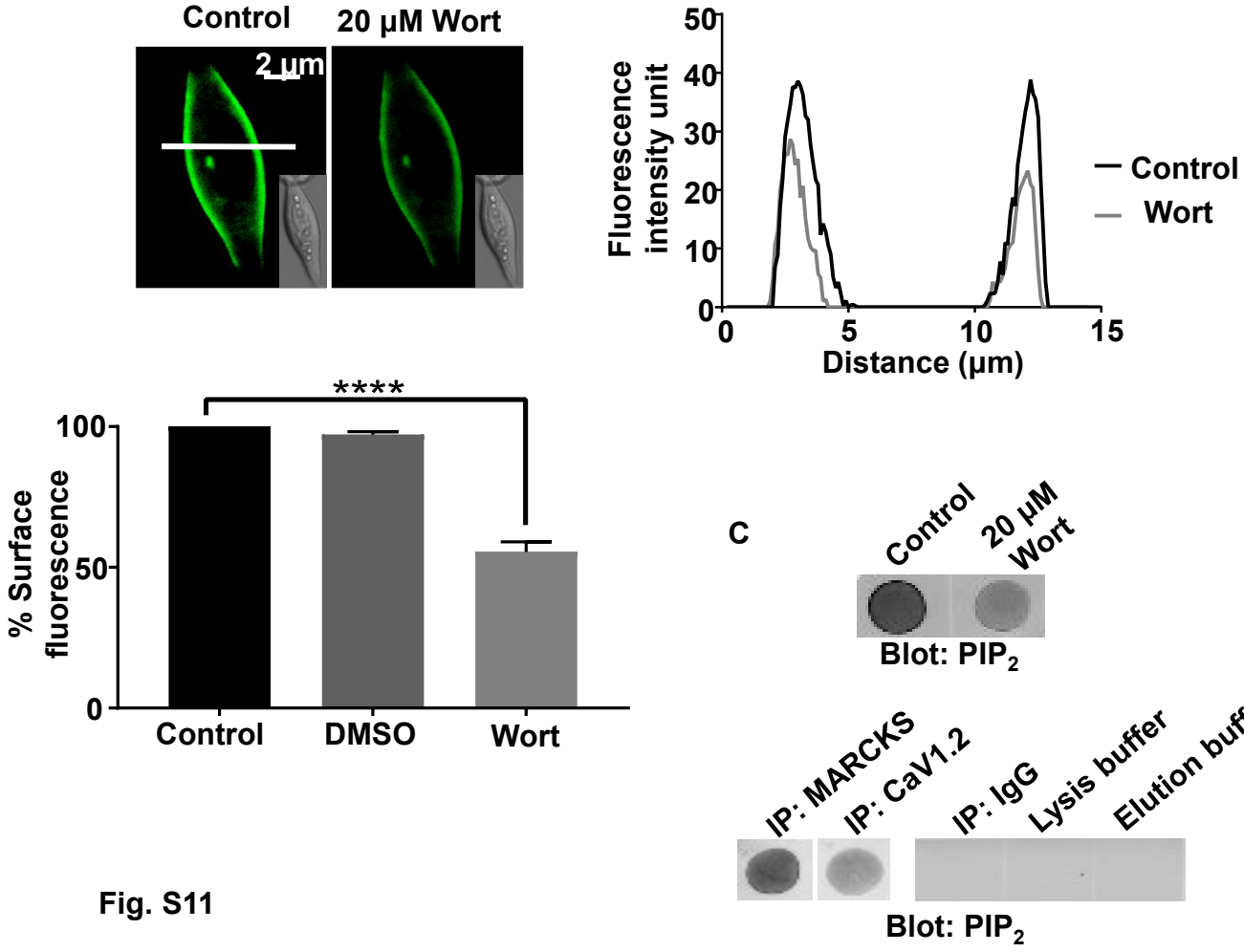
B – GFP-PLCδ-PH
Control
20 µM Wort
2 µm
Fluorescence intensity unit
Distance (µm)
Control
Wort
% Surface fluorescence
****
Control
DMSO
Wort
C
Control
20 µM Wort
Blot: PIP2
IP: MARCKS
IP: CaV1.2
IP: IgG
Lysis buffer
Elution buffer
Blot: PIP2

Fig. S11

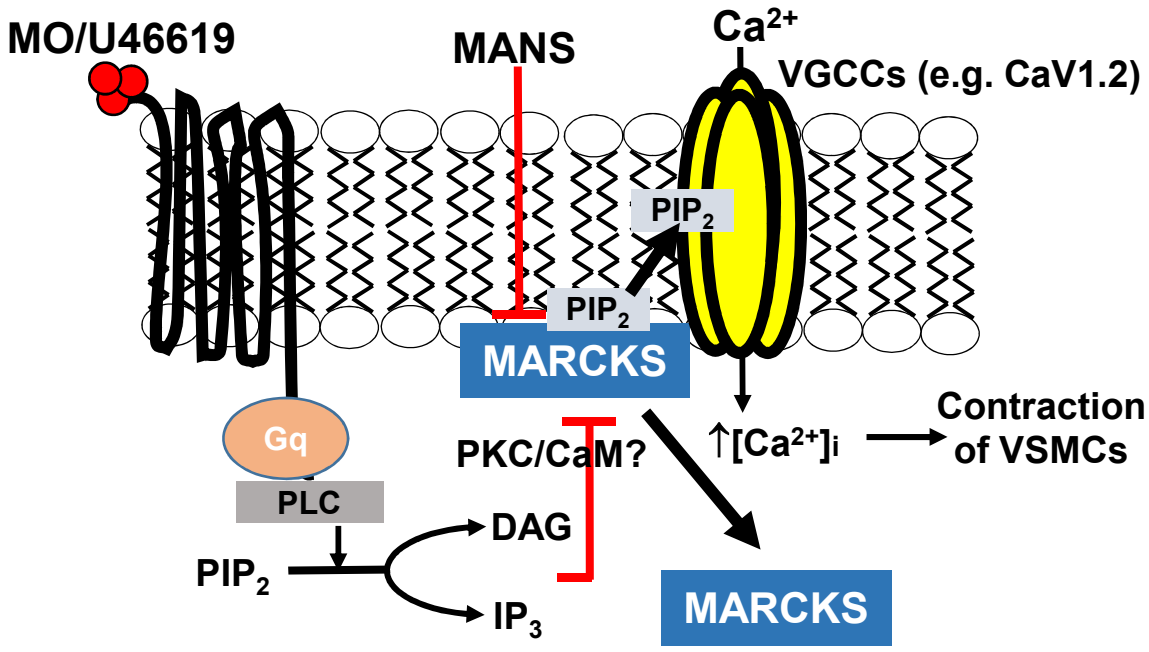
MO/U46619
MANS
Ca2+
VGCCs (e.g. CaV1.2)
PIP2
PIP2
MARCKS
Gq
PLC
PKC/CaM?
↑[Ca2+]i
Contraction of VSMCs
PIP2
DAG
IP3
MARCKS

Fig. S12